NASA CONTRACTOR
REPORT

NASA CR-61188

January 1968

LABORATORY SIMULATION OF THE MARS ATMOSPHERE A FEASIBILITY STUDY

Prepared under Contract No. NAS 8-20082 by
T.S. Chang, W.C. Lucas, and W.W. Youngblood

NORTRONICS - HUNTSVILLE
Northrop Corporation

For

NASA-GEORGE C. MARSHALL SPACE FLIGHT CENTER
Huntsville, Alabama

NASA CONTRACTOR
REPORT

NASA CR-61188

January 1968

NASA CR-61188

LABORATORY SIMULATION OF THE MARS ATMOSPHERE
A FEASIBILITY STUDY

Prepared under Contract No. NAS 8-20082 by
T.S. Chang, W.C. Lucas, and W.W. Youngblood

NORTRONICS - HUNTSVILLE
Northrop Corporation

For

NASA-GEORGE C. MARSHALL SPACE FLIGHT CENTER
Huntsville, Alabama

January 1968 NASA CR-61188

LABORATORY SIMULATION OF THE MARS ATMOSPHERE A FEASIBILITY STUDY

By

T.S. Chang, W.C. Lucas and
W.W. Youngblood

Prepared under Contract No. NAS 8-20082 by

NORTRONICS - HUNTSVILLE
Northrop Corporation

For

Aero-Astronynamics Laboratory

NASA-GEORGE C. MARSHALL SPACE FLIGHT CENTER

FOREWORD

This report presents the results of work performed by Nortronics-Huntsville while under contract to the George C. Marshall Space Flight Center, Aero-Astrodynamics Laboratory (NAS8-20082). The study was performed in response to the requirements of Appendix A-1, Schedule Order No. 17, Technical Directive No. 4, Amendment No. 1. The Responsible Nortronics-Huntsville Engineer was Mr. James T. Stanley and the NASA Technical Coordinator was Mr. D. K. Weidner of the Aerospace Environment Division, Aero-Astrodynamics Laboratory.

Recognition is given to Mr. T. A. Robinson who contributed technical support.

TABLE OF CONTENTS

LIST OF ILLUSTRATIONS

LIST OF TABLES

SUMMARY

The feasibility, from a scientific and engineering design criteria standpoint, of simulating the Martian atmospheric process is considered. Three general areas are studied in detail: simulation of the transportation and deposition of dust and sand by atmospheric processes, dissociation and absorption properties of molecular constituents of the Martian atmosphere, and thermodynamic properties of the Martian atmosphere.

The feasibility of simulating the transportation and deposition of dust and sand under Martian environmental conditions is examined with a view to developing design criteria for Martian missions. The dynamic processes active in the acquisition, transportation, and deposition of unconsolidated material are analyzed and shown capable of producing dust storms and meaningful landforms on the Martian surface.

The basic conditions necessary for the movement of unconsolidated material on the Martian surface are the presence of the material, and winds with velocities high enough to move the material. Consideration of the possible geologic processes active on the Martian surface indicate that volcanic, meteoritic impact, and weathering processes would produce unconsolidated material ranging from clay-size particles to boulders. Theoretical calculations concerning the pertinent dynamic atmospheric processes indicate that threshold velocities one meter above the surface may be as low as 55 m/sec, and that the minimum velocities are for medium-grained sand, which should be plentiful. Previous theoretical studies have predicted peak surface wind velocities as high as 143 m/sec. Thus the transportation and deposition of unconsolidated material on the Martian

surface is shown as a probability. Consideration of the typical landforms composed of wind-blown sand indicates that the classical desert barchan and seif dunes can be expected on the Martian surface, and that their characteristic shapes will reveal much about the wind direction and velocity. Significantly, these features can be observed remotely and their interpretation used to evaluate photographic data returned from probes and to improve design criteria for later missions. Simulation of the acquisition, transportation, and deposition of dust under Martian environmental conditions is considered feasible within the present state-of-the-art, and promises immediate improvement in design criteria.

Theoretical and experimental work on the composition and chemical phenomena of the Martian atmosphere, including spectroscopic data and Mariner IV results, are reviewed and interpreted for their pertinence to atmospheric composition. It is concluded that, although CO_2 is the chief constituent, some water vapor is present. The limited information available on the composition of the Martian atmosphere has been obtained by analogy with the Earth's atmosphere, of which we know a great deal. Numerous ionization and recombination processes, which may interact and affect the transport of the constituents to different layers of the Martian atmosphere, are discussed. The effect of solar corpuscular radiation, as well as electromagnetic radiation, upon these processes may be substantial.

The feasibility of obtaining information related to the Martian atmospheric composition by simulating the atmosphere of Mars in an absorption tube is studied. The physical requirements for such an experiment and an existing multiple-reflection absorption tube system are briefly discussed.

The thermodynamic properties of the Martian atmosphere are reviewed, with consideration given to the vertical profiles of composition, temperature, number density, and pressure. There are major uncertainties in these profiles; in particular, a significant area of disagreement resides in identifying the main ionospheric layer measured by the Mariner IV occultation experiment as being analogous to a terrestrial F_2, F_1, or E layer. The latest values of the optical properties of the atmosphere and surface, the thermal properties of the surface, and the convective heat transfer coefficient of the atmosphere near the surface are briefly reviewed and compared.

A brief discussion of potential experiments is given, which includes polarization studies of CO_2 and H_2O frosts, determination of the upper atmospheric reaction rate coefficients for temperatures approaching 80°K, and determination of the convective heat transfer coefficient near the Martian surface.

SECTION I
INTRODUCTION

The primary objective of this investigation was to review accrued knowledge to date, and investigate the feasibility, from a scientific and engineering design criteria standpoint, of obtaining further Martian atmosphere information through simulation of the Martian atmosphere.

It is readily apparent that the various aspects of a planetary atmosphere are interdependent to the extent that the definition of any one portion requires considerable knowledge of the other portions. While this interdependence broadens any investigation and discourages independent treatment of any portion of particular interest, it permits the study of one portion as an approach to understanding another more pertinent portion on which data are lacking or more difficult to acquire. For example, dust clouds and eolian (wind) landforms are both lower atmosphere products that can be observed remotely and interpreted prior to a venture into the atmosphere itself. The lower atmosphere, in turn, relates to the upper atmosphere and other aspects that may be of more interest in a particular problem.

Recognition of the interdependence of the various aspects of the atmosphere led to the study of three general areas, with some overlap in the subject matter. The areas studied include: Simulation of The Transportation and Deposition of Dust and Sand by Atmospheric Processes, Dissociation and Absorption Properties of Molecular Constituents of the Martian Atmosphere, and Thermodynamic Properties of the Martian Atmosphere. No attempt was made to present a most probable

Martian atmosphere model; therefore, some difference in data may be noted, particularly in overlapping areas, which reflect the different literature sources and emphasize the need for experimentation.

Sections II, III, and IV present the results of the three study areas, while Section V of this report summarizes the results of the three studies and presents recommendations for further theoretical and experimental studies.

SECTION II

SIMULATION OF THE TRANSPORTATION AND DEPOSITION OF DUST AND SAND BY MARTIAN ATMOSPHERIC PROCESSES

2.1 GENERAL

Present estimates of wind velocities, circulation patterns, and related atmospheric phenomena on Mars are based on observations from Earth, and the results of sparse theoretical studies. These estimates, however, are no more than broad approximations and there is a definite need for improvements to meet the design criteria requirements for Martian missions. Some improved estimates are expected through further Earth-based observations, better theoretical techniques, and planetary probe data; however, more immediate and reliable gains can be made through vacuum chamber and wind tunnel simulation of the Martian atmospheric processes. Such simulation studies can contribute much to developing empirical and theoretical techniques, particularly for exploring the interrelationships between the atmosphere and surface materials. The nature of an atmosphere, terrestrial or planetary, governs the effectiveness of weathering, wind erosion, and deposition. In turn, dust clouds and eolian (wind) landforms, which may be observed remotely, are products of atmospheric processes and surface geologic characteristics. Thus, the dust clouds and eolian landforms are important because they can be observed remotely and interpreted for what they reveal of the related atmospheric processes.

This study considers the previous experimental and theoretical work on the transportation and deposition of sand and dust by atmospheric processes as a point of departure, then develops the applicable theories to the point necessary to determine the feasibility of meaningfully simulating those processes of the Martian atmosphere.

A brief review of the physics of eolian processes is made from which appropriate theories are developed to determine whether unconsolidated material exists on the Martian surface, and whether the winds could have velocities high enough to move the material. The determination includes consideration of horizontal, vertical, and cyclonic (dust devil) winds as possible transporting agents. Sand dunes, as typical eolian surface features, are reviewed and their shapes related to winds as a means of determining the atmospheric significance of eolian surface features.

In addition, the types of facilities necessary to simulate the various atmospheric processes are investigated and summarized.

2.2 PHYSICS OF EOLIAN PROCESSES

The problem of particle movement in air or in fluids, in general, has been studied to great depth only in limited areas to meet the needs of a particular discipline or problem. The deposition of silt and sand in rivers and harbors, rock ingestion in jet engines, pipeline transportation of particles, determination of the geological history and formation of sedimentary rocks, and the interpretation of eolian landforms are just a few of the areas that have been investigated. Only in two areas have comprehensive investigations been made: the acquisition, transportation, and deposition of sand (0.1 - 1.0 mm diameter) in a desert environment (ref. 2-1); and the rate of fall of individual particles through a fluid at rest (refs. 2-2 and 2-3). In both areas, theoretical and experimental approaches were used. The laboratory investigations of sand movement (ref. 2-1) were supplemented by field investigations.

Bagnold's studies (ref. 2-1) are of particular interest because they show that a combined theoretical and experimental program can reasonably predict the behavior of spherical, sand-size particles under various wind conditions. His work is quite extensive, covering such areas as: the various factors influencing the acquisition of particles (particle characteristics, wind direction and velocity, surface characteristics, gravity, etc.); transportation of particles (suspension, saltation, and surface creep); and deposition of the particles (true sedimentation, accretion, and encroachment).

An extensive investigation of the physics of particle movement in the Martian environment was not undertaken in this study; rather, only those areas are discussed that would furnish clues as to the probability of movement of sand and dust by Martian winds and that would aid in determining the test requirements of a simulation facility.

Two basic conditions must be met before the movement of sand and dust can take place on Mars: the presence of unconsolidated material, and winds with velocities high enough to move the material. The presence of unconsolidated material on the Martian surface was established in reference 2-4. The existence, abundance, and characteristics of the unconsolidated material are discussed in the following paragraphs. The quantity and characteristics of the unconsolidated material are directly related to the rock types present and the geologic processes active on the surface. Typical rock types expected to be found on the Martian surface are basalt, andesite, obsidian, stoney-iron meteorites, etc. Three geologic processes

are readily seen as sources of unconsolidated material. These processes are volcanism, meteoritic impact, and gradation.

Unconsolidated material formed during meteoritic impacts and volcanic eruptions should closely resemble that found on Earth; however, this is not thought to be true in the case of sediments formed by Martian gradation processes. On Earth, chemical weathering, physical weathering, and a variety of erosional agents (water, wind, ice, etc.) are active. Water, through erosion and chemical weathering, is the dominant influence in determining the characteristics of most terrestrial sediments, in particular, the formation of clay-size particles. The apparent absence of large amounts of water indicates that while clay-size particles (<0.0039 mm) may be present, the extent and quantity will be much less than found on Earth.

It has been generally accepted (refs. 2-5 and 2-6) that the Martian surface is comparatively smooth when compared to the Earth. Ryan, in his paper concerning Martian yellow clouds, (ref. 2-7) considered the maximum grain diameter of surface material to be no greater than 100μ and probably no greater than 50μ. This conclusion appears unjustified when careful consideration is given to the possible Martian geologic processes. Volcanism and meteoritic impacts would produce unconsolidated material ranging from clay-size particles to boulders. Also, physical weathering would generally produce coarse-grained material, with the actual grain size determined largely by type and texture of the parent rock. Grain sizes as large as 2 to 4 mm should not be uncommon. The unconsolidated material furnished by these sources then would be transported and deposited over much of the planet's surface by eolian processes. Thus, it has been concluded by the authors that unconsolidated material may be wide-

spread on the Martian surface and that the material may occur as well- to poorly sorted sediments. The well-sorted sediments are expected to consist mostly of clay- and sand-size particles, while the poorly sorted sediments may include particles ranging from clay sizes to boulders.

Large-scale eolian landforms are commonly classified as regs or ergs. Regs are erosional features where the fine-grained material has been removed, leaving an area composed primarily of coarse-grained material. Ergs are depositional features, generally described as sand seas, and may contain a large variety of land forms depending on the amount of sand available and the velocity and direction of the winds. An additional depositional feature would be deposits of fine-grained material similar to terrestrial loess deposits. Regs, ergs, and loess deposits are basically end products of the eolian processes. Martian desert areas will probably contain features in various stages of development. It is expected that Mars will have large amounts of unconsolidated material exposed on its surface. This material may range from well-sorted to poorly-sorted sediments. Grain size will be variable; clay- and sand-size particles for the well-sorted sediments, and clay-size particles to boulders for the poorly sorted sediments.

Winds with velocities high enough to move the unconsolidated material and form sand and dust clouds also appear to be present on the Martian surface. Yellow clouds have been observed on the Martian surface, usually in the lower latitudes and predominantly in the southern hemisphere. The clouds are generally local in extent and dissipate in a matter of days. However, there have been occasions (1956) when the entire disc was covered for several weeks. The results of

photometric and polarization studies imply that the yellow clouds are composed of solid particles.

The velocities of these cloud movements have been measured telescopically (accuracy ± 25 percent) on numerous occasions (ref. 2-8). The maximum velocity, observed in 1956, was 24.69 m/sec. Numerous other measurements have shown velocities in the 10 to 12 m/sec range. As on Earth, it is probable that winds within the clouds are higher than the velocity of the cloud movement itself. Theoretical studies have produced estimates of peak surface wind velocities as high as 143 m/sec (ref. 2-9).

Two types of phenomena may be responsible for the movement of unconsolidated material on Mars. These are horizontal and vertical winds associated with large-scale climatic disturbances and small-scale cyclonic systems (dust devils).

2.2.1 Horizontal and Vertical Winds as Agents for Transporting Martian Unconsolidated Material

Only a few investigators have approached the problem of sand and dust movement on Mars from a theoretical point of view in any degree of detail. Ryan (ref. 2-7), using 25-mb and 80-mb atmosphere models, discussed the winds required to initiate grain motion and to maintain them aloft, range of particle sizes that may make up dust and sand clouds, and the probable result of the depositional phase of the eolian processes. A JPL document (ref. 2-8) basically updates the Ryan paper by recalculating many of the results using pressure values of 14 mb and 40 mb.

Ryan's conclusions concerning Martian threshold velocities are the results of calculations based on Bagnold's fluid threshold equation. The

calculations made in this report are also based on this basic equation and the numerical data in Table 2-1. Bagnold's fluid threshold equation is given as:

$$v_t = 5.75A\sqrt{\frac{\sigma - \rho}{\rho} gd} \log \frac{z}{k} \quad (1)$$

where:

v_t = Threshold fluid velocity at any height

A = Dimensionless parameter

σ = Particle density

ρ = Atmospheric density

g = Gravity field strength

d = Particle diameter

z = Height above the ground

k = Roughness factor ($\simeq$ 1/30 the effective grain diameter).

This equation may also be stated as:

$$v_t = 5.75\ V_{*t} \log \frac{z}{k} \quad (2)$$

where V_{*t}, the threshold velocity gradient, is equal to:

$$A\sqrt{\frac{\sigma - \rho}{\rho} gd} \quad (3)$$

Bagnold found experimentally that the dimensionless parameter "A" was primarily dependent on the Reynolds number. The Reynolds number (Re) is defined as:

$$Re = \frac{(\text{velocity } V_{*t})(\text{size dimension d})}{(\text{kinematic viscosity } \gamma)} \quad (4)$$

The critical Reynolds number value was found experimentally to be 3.5. For particles with Reynolds numbers greater than 3.5, A is almost constant. In the air on Earth this value of A is approximately 0.1. For particles with Reynolds numbers less than 3.5, the value of A, which was found by Bagnold, is not constant.

No experimental work has been performed under Martian environmental conditions to determine values of A. To overcome this, it is assumed in this report that the fluid threshold equation is valid for Mars and that the dimensionless parameter A for Mars (A_m) is approximately equal to the dimensionless paramater A on Earth (A_e) for a given Reynolds number. The Reynolds number to coefficient A_e relationships were calculated using equations (3) and (4) from data found in reference 2-1. The Re to A_m to d relationships for Mars were then determined by the following equations:

$$Re = \frac{d}{\gamma} V_{*t} \tag{5}$$

or

$$Re = \frac{d}{\gamma}\left[A\left(\frac{\sigma-\rho}{\rho} gd\right)^{\frac{1}{2}}\right] \tag{6}$$

Equation (5) is solved for d using numerical data for the two atmospheric models given in Table 2-1 and terrestrial values of Re and A. With the relationships between Re, A_m, and d known, the fluid threshold velocities then can be found using equation (1) for various heights above the surface and for different roughness factors.

As discussed earlier, we disagree with the general opinion that Mars is extremely smooth and consider it to be as rough or rougher than the Earth. With this assumption, we calculated the fluid threshold velocities at a height

of one meter above the surface using recent Martian atmosphere data (Model 1 and Model 2 given in Table 2-1). The four different values (0.03, 0.05, 0.1, and 0.2 cm) for the roughness factor (k), which were used in the calculations, represent surfaces composed of particle sizes ranging from 9 to 60 mm in diameter. The results of these calculations are shown in Figures 2-1 and 2-2.

Table 2-1. MARTIAN ENVIRONMENTAL DATA

	GRAVITY (cm/sec^2)	ATMOSPHERE (SURFACE)						
		DENSITY (gm/cm^3)	PRESSURE (mb)	COMPOSITION %		KINEMATIC VISCOSITY (cm^2/sec)	MEAN FREE PATH (m)	COEFFICIENT OF VISCOSITY (kg/m-sec)
				CO_2	N_2			
MODEL 1	375	1.5657	10	50	50	11.0	6.414×10^{-6}	1.7252×10^{-5}
MODEL 2	375	1.2096	4	100	0	9.8	1.020×10^{-6}	1.1827×10^{-5}

The high wind velocities indicated by these calculations are not the minimum wind velocities necessary to cause sand and dust movement on the Martian surface. There exists a critical wind velocity, less than the fluid threshold velocity of a given surface, where saltation, once set in motion, can just maintain itself indefinitely down-wind of the disturbance. This critical velocity was termed by Bagnold as the "impact threshold velocity." Baynold's experimental results show that impact threshold velocities are approximately 20 percent lower than those for the fluid threshold. Assuming the validity of this phenomenon for Mars, the minimum impact threshold velocity based on the data in Table 2-1 is approximately 55 m/sec. Considering the possibility of a high gust of wind, an earthquake, meteor impact, landslide, etc., originating the saltation of particles, it is

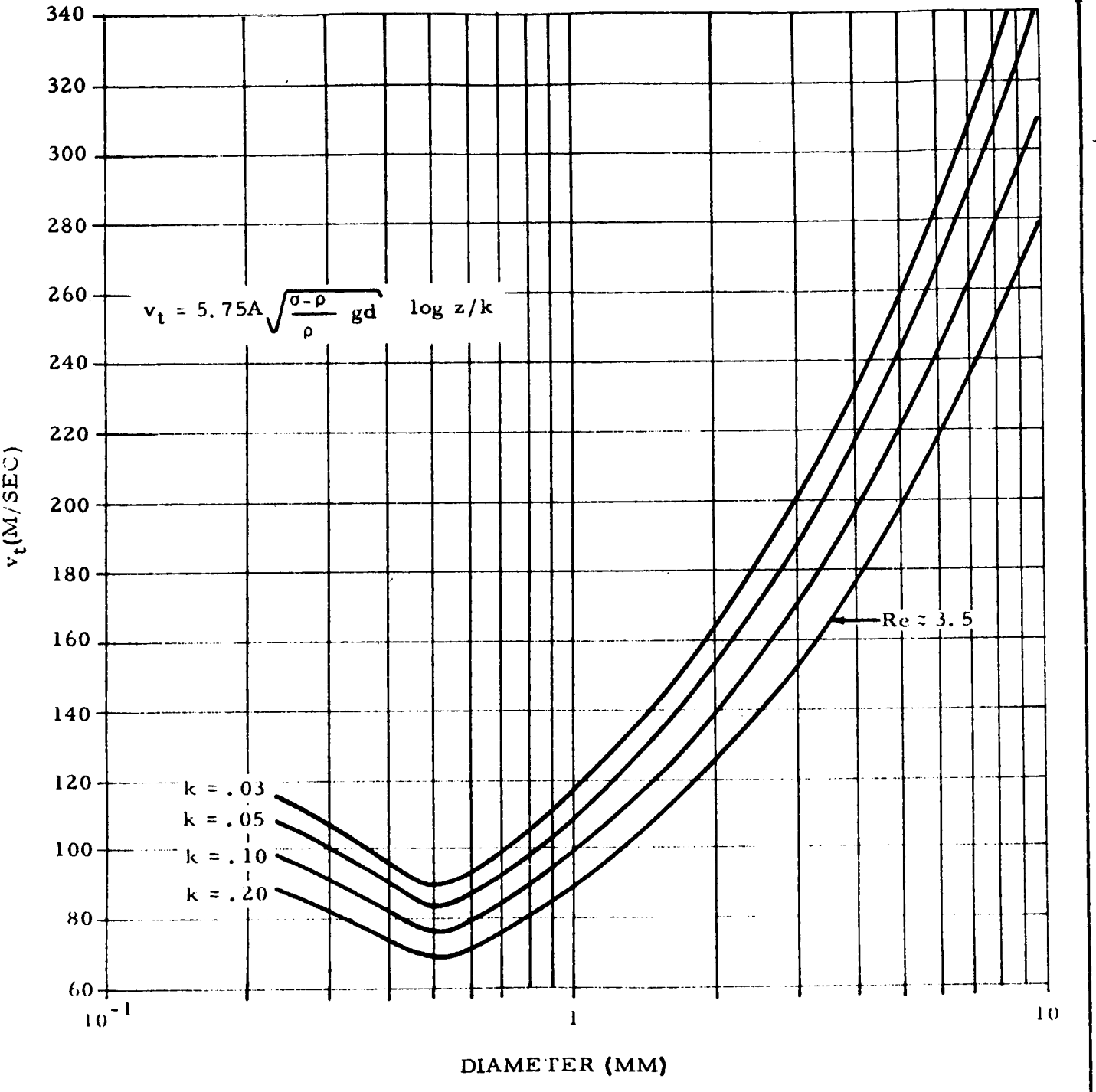

Figure 2-1. FLUID THRESHOLD VELOCITY AS A FUNCTION OF PARTICLE SIZE FOR ATMOSPHERE MODEL 1 AT A HEIGHT OF ONE METER ABOVE THE SURFACE

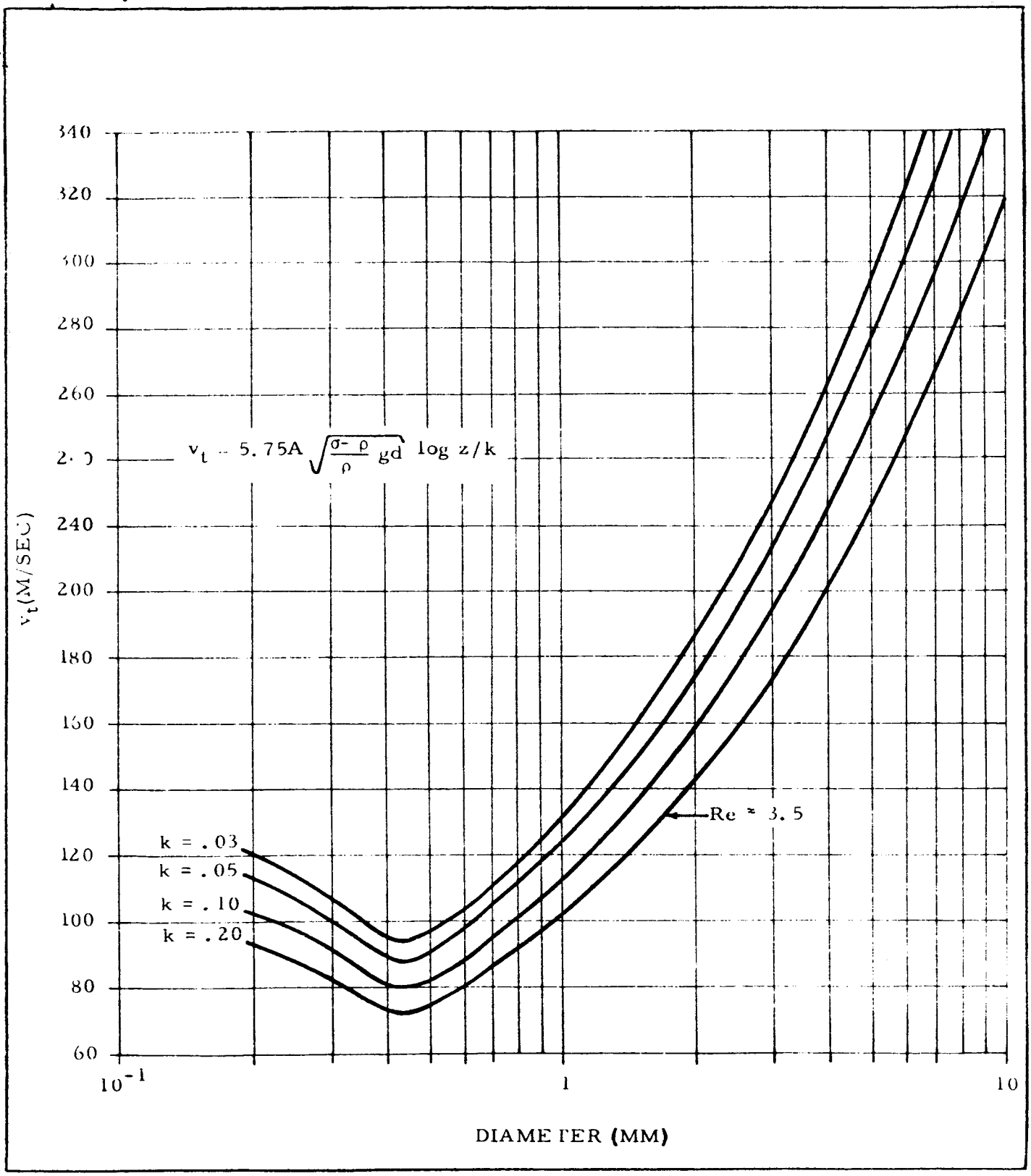

Figure 2-2. FLUID THRESHOLD VELOCITY AS A FUNCTION OF PARTICLE SIZE FOR ATMOSPHERE MODEL 2 AT A HEIGHT OF ONE METER ABOVE THE SURFACE

possible for these movements to grow into dust or sand storms and to form eolian landforms. Additional calculations by the authors to determine the effect of grain density on the fluid threshold velocities showed that the difference in densities between feldspar (2.5 g/cm^3) and pyroxene (3.6 g/cm^3) had little influence on the fluid threshold velocity of a particular surface. However, while the fluid threshold velocity is practically unaffected, the impact threshold velocity may be noticeably lower. This possibility, however, has not been confirmed and will require additional study.

The vertical winds required to keep particles aloft must be considered along with the fluid threshold velocities required to initiate particle movement. Using the Cunningham-Stokes equation for particles less than 10μ, the Stokes equations between 10 and 100 μ, and graphically solving for particles greater than 100 μ, Ryan (ref. 2-7) determined that vertical wind velocities required to maintain particles aloft on Mars are less than for Earth over a large range of grain sizes (1 to 300 μ for an atmospheric pressure of 80 mb, and 4 to 200 μ for 25 mb).

Using Models 1 and 2, we recalculated these vertical wind velocities showing (Figure 2-3) that even with a 4-mb atmosphere, particles ranging in size from ~14μ to ~140 μ in diameter will require lower vertical wind velocities on Mars than on Earth.

The significance of these calculations is seen when the probable Martian surface and environmental conditions are considered. The unconsolidated material on the Martian surface is believed to be typically composed of a wide range of grain sizes resulting from the action of volcanic, meteoritic impact,

and gradation processes. Assuming such a surface and a Martian wind with velocities great enough to initiate and sustain movement of grains 0.4 to 0.6 mm in diameter, it is logical that clay-size particles present will be dislodged and carried into the atmosphere. Once these small particles are air-borne, their settling rates, implied by the vertical wind velocities shown in Figure 2-3, will be similar to and in some cases less than on Earth.

From the results of the preceding calculations and discussion, it appears that Martian atmospheric and surface conditions will be conducive to the formation of both dust clouds and eolian surface features.

2.2.2 Dust Devils as Agents for Transporting Martian Unconsolidated Material

The yellow clouds on Mars have been explained in several ways. The major explanations for the existence of the yellow clouds are major meteoric collisions (ref. 2-10), horizontal wind storms (ref. 2-7), and small-scale cyclonic disturbances such as tornadoes and dust devils (refs. 2-10, 2-11, and 2-12). Since the area of concern in this final report is the feasibility of Earth-based simulations of Martian atmospheric features, the meteoric collision theory will not be considered.

Measurements of terrestrial dust devils have been taken by Ives (ref. 2-13) and Sinclair (ref. 2-14). Sinclair observed high horizontal and vertical wind velocities near the ground in the terrestrial dust devils. Similarly, Ives observed the transport of large amounts of dust to high altitudes through the agency of dust devils. This has been used by Neubauer (ref. 2-12) as a strong argument for proposing that small-scale cyclonic wind systems are a possible explanation for the yellow clouds.

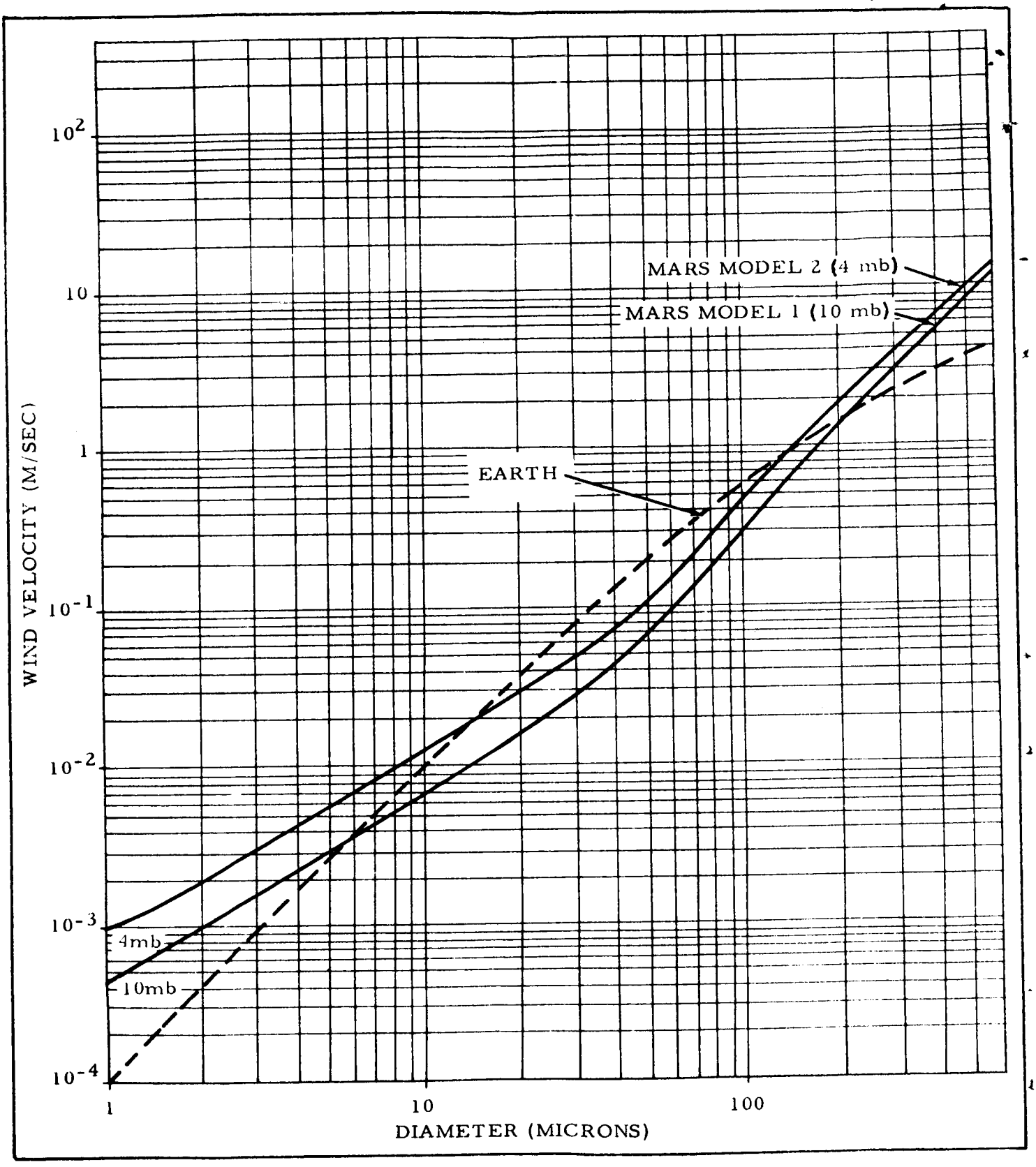

Figure 2-3. MINIMUM VERTICAL WIND VELOCITIES NECESSARY TO MAINTAIN PARTICLES ALOFT AS A FUNCTION OF GRAIN SIZE

Neubauer (ref. 2-12) proposed that "...small-scale cyclonic wind systems can explain the formation of dust clouds, even in the abscence of strong large-scale wind systems". He proceeded to calculate the time-dependent vertical temperature profile for the region very close to the Martian surface. The results of this calculation indicate "...a very steep temperature gradient near the ground around the time of the temperature maximum."

Neubauer extended his analysis to the mechanism of the dust devils which he described as follows:

> "The hot air from the ground in the dust devil chimney has a smaller pressure decrease with height than the surrounding cold air. To fit the external pressure at the upper end of the dust devil there must be a reduced pressure at the ground. The force resulting from the pressure gradient and the buoyancy force accelerates the hot air in the lower part of the chimney. A sudden collapse of the reduced pressure core is inhibited by the centrifugal forces of the rotating air masses."

Neubauer's analysis of the dust devil is based on a simple integration of the equation of motion from the Martian surface to the top of the dust devil. The major relationship resulting from the analysis was the maximum wind velocity at the top of the dust devil

$$v_{max}^2 = 2g\Delta T_o / \bar{T}_o b \qquad (7)$$

where g is the acceleration of gravity ($\sim$ 375 cm/sec^2 on Mars), ΔT_o is defined as $T_o - \bar{T}_o$, T_o is the surface atmospheric temperature, $\bar{T}_o$ is the daily mean surface atmospheric temperature, and b is proportional to 1/D where D is the dust devil diameter. By analogy to Earth dust devils, Neubauer obtained the relationship $bD \simeq 4/15$ and, therefore,

$$v_{max} \simeq 2.5(gD\Delta T_o/\bar{T}_o)^{\frac{1}{2}} \qquad (8)$$

This relationship is plotted in Figure 2-4 for the conditions of the Martian atmosphere. However, the results of Neubauer should be checked since he assumed the main constituent of the Martian atmosphere to be nitrogen rather than the now generally accepted carbon dioxide.

Thus, according to Neubauer, "...the critical parameter for the wind velocities in a dust devil is $g\Delta T_o/\bar{T}_o$. Furthermore, one would expect the number of dust devils created per unit area and unit time to increase as $\Delta T_o/\bar{T}_o$ increases." To support his argument for the enhanced occurrence of dust devils on Mars, Neubauer calculated a $\Delta T_o/\bar{T}_o$ of 0.21 for the maximum value resulting from his analysis of the temperature profile near the ground and compared this value with a typical value for Earth of 0.12 (given by Ives, ref. 2-13). This comparison shows that the initiation of dust devils should occur more easily on Mars than on the Earth.

Ives (ref. 2-13) and Sinclair (ref. 2-14) suggest that the up-currents of dust devils can reach very high altitudes, as high as 5 to 9 km which is the altitude where dust clouds have been observed on Mars (ref. 2-15).

Tang (ref. 2-11) calculated the maximum surface wind speed on Mars that might exist in a storm. He suggested that the maximum surface wind velocity on Mars would be found in a tornado, assuming that such storms could exist. The calculations were based on a formula for the maximum surface wind velocity for a convective vortex as derived by Kuo (ref. 2-16)

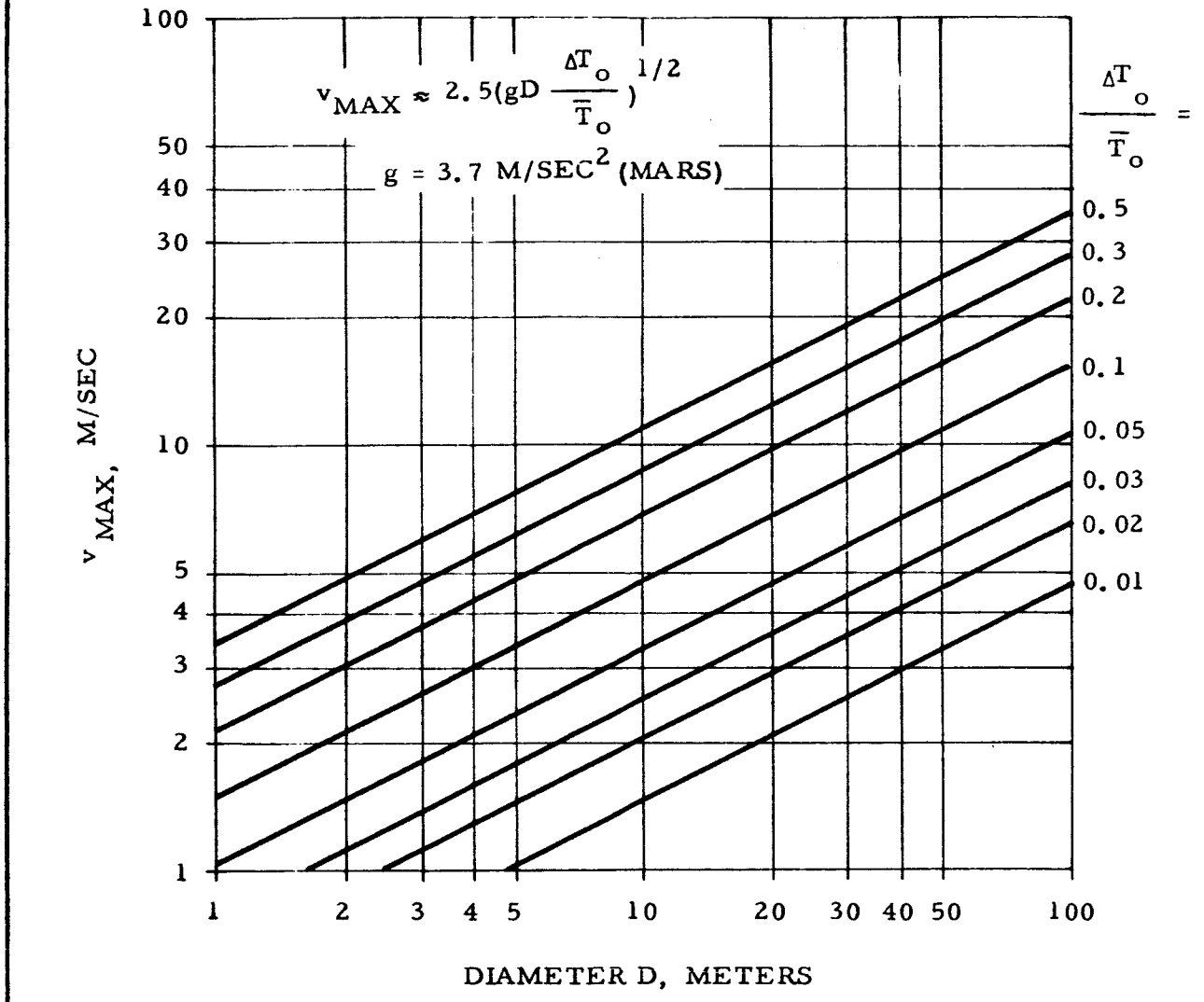

Figure 2-4. MAXIMUM VELOCITY AT THE TOP OF A DUST DEVIL AS A FUNCTION OF ITS DIAMETER

$$V_{max} = \gamma R T_o \left\{ \frac{2}{\gamma - 1} \left[1 - \left(\frac{p_c}{p_o} \right)^k \right] \right\}^{\frac{1}{2}} \quad (9)$$

where V_{max} = Maximum tangential velocity

γ = The ratio of specific heat at constant pressure to that at constant volume

R = Gas constant for the atmosphere

p_c = Surface pressure at the center of the vortex (central pressure)

p_o = Surface pressure at a distance where the wind velocities are nil (surrounding pressure)

k = Poisson constant = $(c_p - c_v)/cp$

T_o = Surface temperature.

Tang obtained a maximum surface wind velocity of 114 m/sec in the vortex of a Martian tornado when assuming a surface pressure of 25 mb and a pressure drop to the center of the vortex of 2 mb. It was concluded from this that a slight disturbance on Mars can cause a severe storm.

2.3 SIGNIFICANCE OF EOLIAN SURFACE FEATURES

Interpretation of present or past climatic conditions from eolian surface features is common in geological analysis and should be applicable to a better understanding of the Martian and other planetary atmospheres. Numerous studies have been made concerning conditions and factors entering into the formulation of ripples, dunes, sand sheets, and other related eolian phenomena. Again, as in the physics of particle movement, comprehensive studies of these problems should consist of theoretical, experimental, and field approaches.

Sand ripples have interested scientists for many years and explanations for their existence and physical characteristics are controversial. Early attempts assumed that the formation of eolian and fluvial sand ripples were analogous. The results of experiments showed that the similarities between the two types of ripples are superficial, and fundamental differences exist in the processes and conditions under which they are formed.

Bagnold (ref. 2-1) recognized that combinations of a number of factors were responsible for eolian sand ripples. These were: wind, saltation, size of surface grains, surface relief, and the state of sand movement (erosional or depositional phases). These factors are mutually interactive and therefore underlie the numerous interpretations of the ripple phenomena.

Recent work by Sharp (ref. 2-17) concludes that ripple dimensions (height, wave length, and index) are controlled by the size of grains traveling by surface creep and wind velocity. He found that the degree of asymmetry of individual sand ripples varies inversely with wind velocity and directly with grain size. Of particular interest were Sharp's observations of the rate of movement of ripples. Under wind velocities ranging from 16 to 40 mph, ripples were observed to move at velocities of 0.35 to 3.2 inches per minute. By observing the rate of movement of a particular ripple, the wind direction can be determined; and wind velocity and ripple particle size can be calculated if values are known for one of them. The possibility of applying this approach to observations made from a Mars surface lander is intriguing.

Of the large-scale eolian features, sand dunes are the most valuable in determining present climatic conditions. Their shapes, sizes, and rates

of movement are indicative of wind direction and velocity. Careful analysis of aerial photographs of sand dunes not only can supply information concerning the winds that formed the dunes, but may also indicate the characteristics of the material composing the dunes.

The classical dune shapes develop best in desert regions where wind direction and velocity are the primary controlling factors. Dunes also develop in riverine and coastal areas where other factors enter into their forms. For example, the characteristics of riverine and coastal dunes are greatly influenced by moisture and vegetation which contribute to confused forms. Most dunes, however, are complex features and may occur alone or in groups.

The barchans and seif dunes common to desert regions are perhaps the best known eolian features. The shapes of barchans and seif dunes are illustrated in Figure 2-5. The arrows in the illustration indicate the relative velocities and directions of the shaping winds.

The barchan, for example, is indicative of a moderate wind with a nearly constant direction. The well-developed barchan is a crescent-shaped feature with the horns trailing off downwind. These dunes are usually migratory and range in size from a few meters to 90 meters in height and up to 400 meters across. Rates of movements as high as 50 feet per year have been measured. Bagnold, using his wind tunnel experiments as a basis, formulated the following equation for predicting the forward movement of barchans:

$$C = \frac{q}{\gamma H} \qquad (10)$$

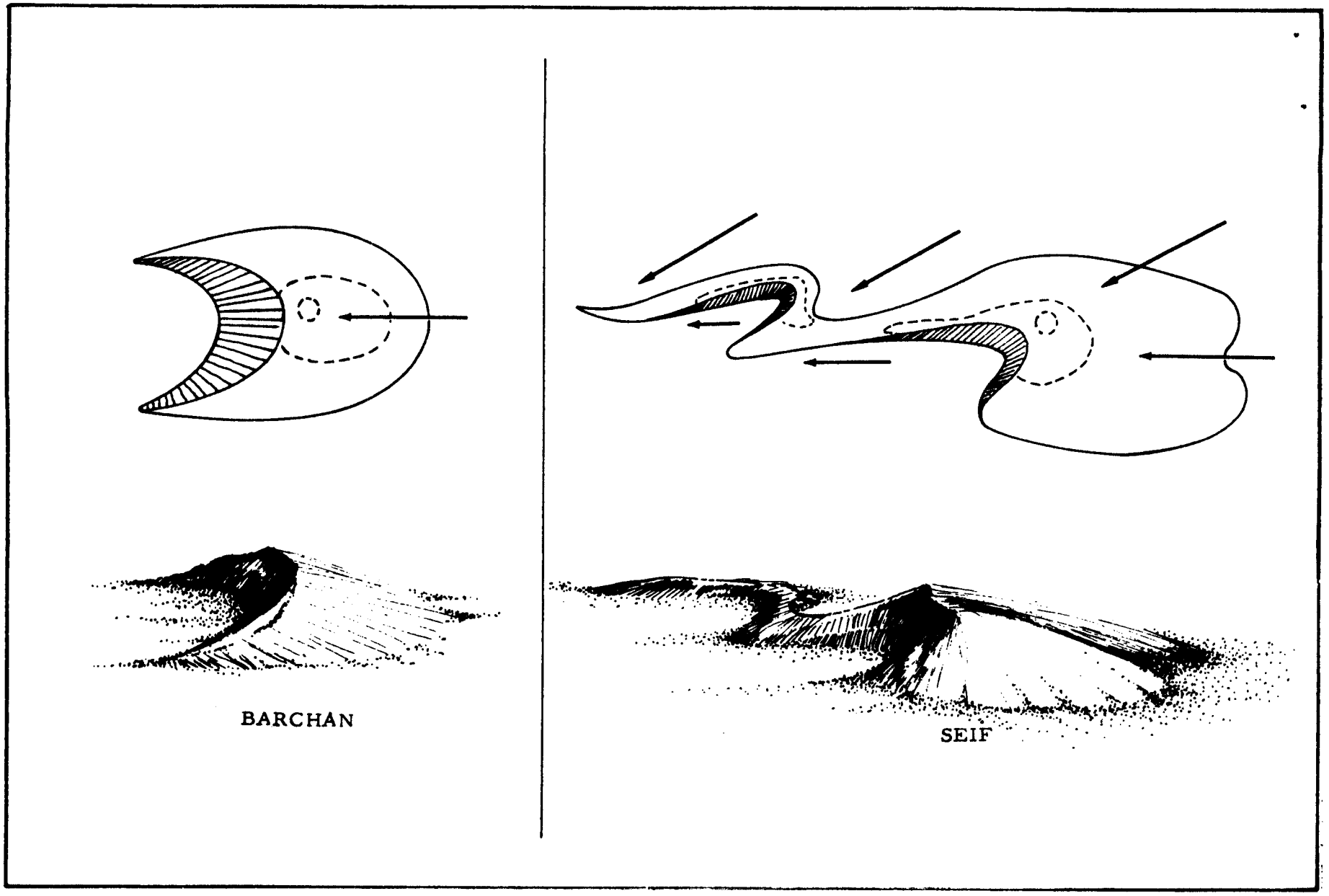

Figure 2-5. WIND DIRECTION AND VELOCITY RELATED TO THE FORMATION OF BARCHAN AND SEIF DUNES

where:

C = Displacement (m/hr)

γ = Bulk specific gravity of the sand (tons/m^3)

H = Height of the dune (m)

q = Rate of sand transportation by the wind (metric tons/linear meter/hr).

The rate of sand transportation (q) is defined as:

$$q = 1.5 \times 10^{-9}(v - V_t)^3 \qquad (11)$$

where:

v = Effective wind velocity at heights z(m/sec)

V_t = Threshold velocity (m/sec).

The results of field studies have generally confirmed the validity of Bagnold's equations. A striking example was the result of field studies made in Peru by Finkel (ref. 2-18). A comparison by Finkel of the measured annual barchan displacement and the predicted displacement by the Bagnold theory is shown in Figure 2-6.

Seif dunes, shown in the simplified form in Figure 2-5, are relatively large surface features. The largest extend for hundreds of miles and may reach heights as great as 200 meters. The dunes line up approximately parallel to the prevailing wind and therefore are often referred to as longitudinal dunes. The wind directions shown in Figure 2-5 reflect Bagnold's concept of the growth of seif dunes. He maintained that two winds were involved in the formation of the dunes. A prevailing gentle wind parallel to the trend of the seif chain is responsible for the lengthening of the chain. Sand-bearing storm winds blowing out of a single quarter controlled the height and width of the dunes.

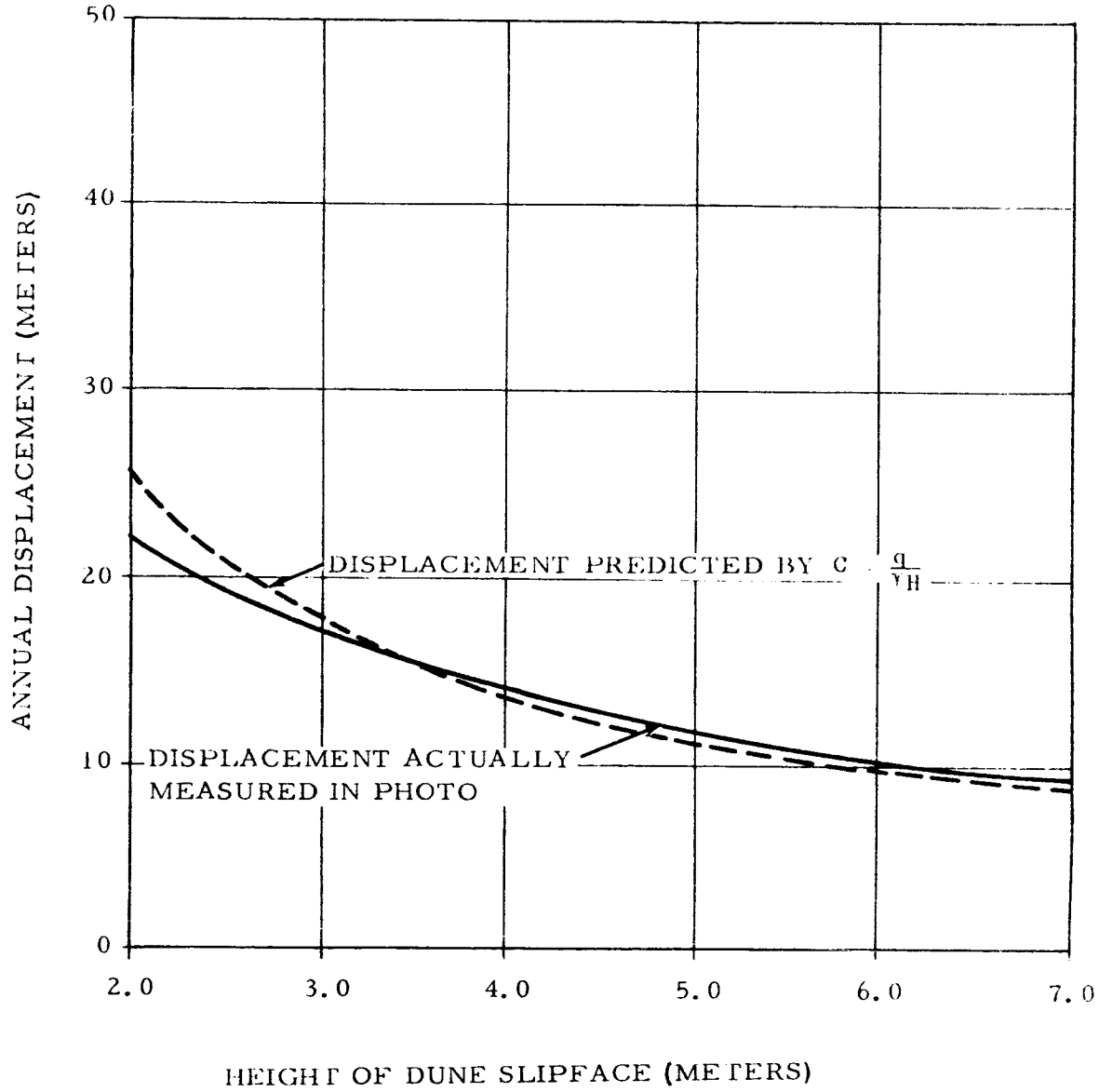

Figure 2-6. ANNUAL BARCHAN DISPLACEMENT MEASURED AND PREDICTED BY THE BAGNOLD THEORY (After Finkel)

Assuming the availability of source material and the presence of high-velocity winds, it appears reasonable that barchan, seif, and complex dunes exist on Mars. Analysis of photographs of Mars obtained by spacecraft could supply valuable information concerning the direction and velocity of surface winds. Experimental studies, under Martian and terrestrial environmental conditions, would improve our knowledge of the physics of eolian processes and should greatly improve the accuracy of photographic interpretations of the Martian surface as an indication of climatic conditions.

2.4 SIMULATION FACILITIES

Simulation experiments are a necessary part of any comprehensive study of eolian processes. The results of analysis of eolian processes and the problem of interpreting eolian landforms indicate that two types of simulation facilities would be desirable: a horizontal wind facility capable of simulating both terrestrial and Martian environments for studying the acquisition, transportation, and deposition of rock fragments; and a facility for simulating terrestrial and Martian dust devils.

2.4.1 Horizontal Wind Facilities

Before the problem of Martian eolian processes can be approached with confidence, it is necessary to increase our knowledge of eolian processes on Earth. Investigators, particularly Bagnold, have shown the feasibility of wind tunnel experiments from both a scientific and engineering point of view when the experiments are coupled with both theoretical and field studies.

In recent years the advancements in simulation technology and measuring techniques make it possible to improve the accuracy and to expand the scope of earlier studies to include a large variety of samples (density, size, shape, etc., of particles) and environmental conditions.

Little simulation work has been performed to date in the study of Martian eolian processes; however, some preliminary simulation was performed by Hertzler, et al., (ref. 2-19). These studies were concerned mainly with threshold velocities required to pick up various types of dust, and with the resulting abrasion on some selected surface coatings. However, the facilities used did not permit adequate studies to fully define the flow field. The velocity gradients, du/dz, were not determined, nor were the particular density profiles. In fact, the flow bed was not long enough to determine whether the flow was fully developed and no mention was made of the surface boundary layer. A longer flow bed also would have permitted (at least qualitatively) an investigation of the particle saltation, surface creep, rate of particle movement, and small-scale surface features.

2.4.1.1 Terrestrial Wind Simulation Facility. The design requirements of a facility to simulate terrestrial dust storms must be considered first. The physical requirements are far easier to meet in the case of a terrestrial dust storm simulator because the facility may be exhausted directly to the atmosphere. The major design parameters may be listed as follows:

- Flow medium -- air
- Static pressure -- 1 atmosphere
- Wind velocity -- 0 - 100 km/hr
- Test bed temperature -- 240 - 328°K

- Air (wind) temperature -- 240 - 328°K
- Air (wind) relative humidity -- ≈ 0-100%
- Test section area -- 122 cm x 122 cm
- Test section length -- 12.2m (minimum)
- Particle sizes -- $\geq 1\mu$.

The suggested facility size is based only on preliminary estimates. Final design size would be based on considerations of the boundary layer thickness, attainment of fully developed flow, and, of course, considerations of the overall facility cost. The terrestrial wind simulation facility would be much simpler to design, fabricate, and operate. This is because there is no requirement for vacuum pressures or for recovery of the flow medium. The suggested major components of the facility may be listed as follows:

- Flow conditioning system (including filtration, heating or cooling, and humidification or dehumidification)
- Axial flow fan
- Flow straightening section
- Test bed section (including heating or cooling systems, and monitoring instrumentation).

2.4.1.2 Martian Wind Simulation Facility. Ranges of the design requirements for a facility to simulate Martian dust storms may be listed as follows:

- Flow medium - CO_2 and N_2
- Static pressure - 4 - 25 mb
- Wind velocity - 0 - 200 km/hr
- Particle sizes - $\geq 1\mu$

- Test bed temperature - 175 - 300°K
- Flow medium temperature - 175 - 300°K
- Test section area - 122 cm x 122 cm
- Test section length - 12.2m minimum.

The ranges of requirements were acquired through a review of the latest analytical efforts on the subject. The cost of vacuum pumping equipment capable of handling the required flows may largely dictate facility size. Added to this problem is the increased boundary layer thicknesses that would be experienced by this facility over the facility required to simulate terrestrial dust storms. The problems involved with construction of a Martian wind simulation facility include at least the following:

- Facility must withstand vacuum pressure
- Vacuum pumping system must maintain a relatively large mass flow rate for extended periods of time
- Test section must be large enough to compensate for boundary layer growth
- A pumping system may be required for the recovery and recompression of the special flow medium.

Thus, it is obvious that the design requirements for a facility to simulate the Martian surface winds are far more stringent than the terrestrial simulator.

2.4.1.3 Required Measurements. In order to specify completely the conditions at any position in the facility, it is necessary to determine the local velocity, static pressure, temperature, Reynolds number, and particulate density (concentration of the small particles entrained in the flow). These conditions may be specified by obtaining the following measurements:

- Freestream static pressure, p
- Stagnation pressure, p_o
- Stagnation temperature, T_o
- Sand flow, q
- Particulate density, ρ_p.

Measurements of the pressures and temperature may probably be made with little difficulty by conventional instrumentation (except for the contaminating influence of the dust particles). Determination of the particulate density will be decidedly more difficult. It may be necessary to use flow visualization techniques to obtain useful particulate density profiles. Some methods of determining the particulate densities are listed as follows:

- High-speed motion pictures
- Shadowgraph
- Rake probe.

The high-speed motion pictures, shadowgraph, and similar flow visualization techniques may provide useful information, but will probably give only qualitative results. The rake probe is a possibility for obtaining density profiles of a more quantitative nature. The device shown in Figure 2-7 is only a tentative suggestion and no device of a similar nature has been reviewed in the literature. The idealized system shown in Figure 2-7 is not to be considered as a representation of the actual particle density profiles. However, it is believed that a simple rake, such as shown, could be very useful to the study. Sizing of the probe orifice and screen mesh will depend on the particle grain size, flow stream velocity, and pumping rate of the probe rake system.

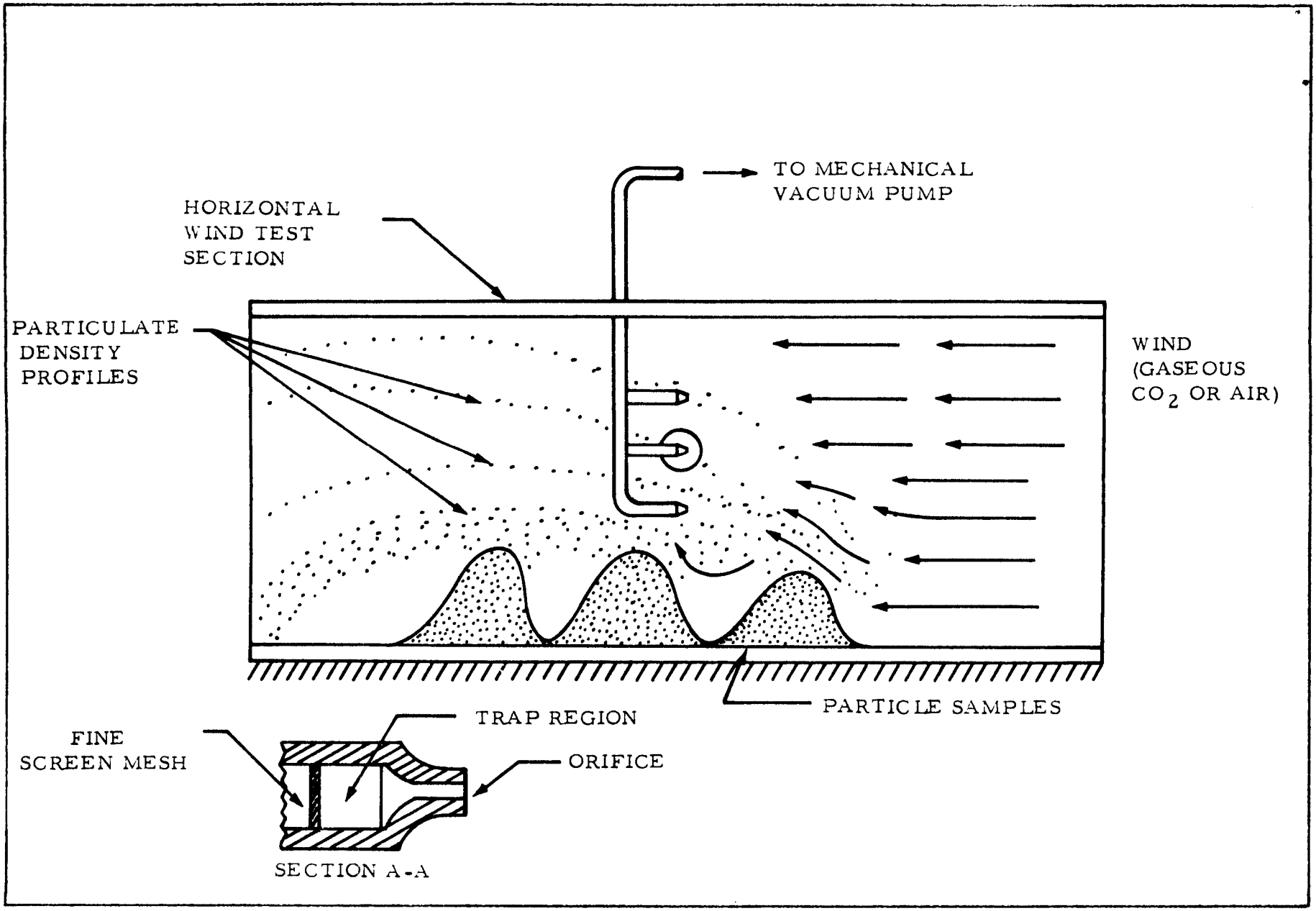

Figure 2-7. PROBE RAKE FOR DETERMINATION OF PARTICULATE DENSITIES

Determination of the remaining flow parameters will involve the use of conventional instrumentation. Entrainment of dust particles will cause some changes in the flow parameters, and measurements of these effects are expected to be relatively difficult for low entrainment rates. High entrainment rates may cause larger changes in the flow field, but will be more difficult to measure due to the abrasive and clogging action of the dust.

2.4.2 Dust Devil Simulation Facility

It appears that an effort should be made toward improving the theoretical analysis of dust devils before the design of a simulation facility, which follows from theory, is undertaken. To accomplish this, the following effects should be included in Neubauer's analysis:

- Surface friction
- Influence of the dust content of the air on the dynamics of the dust devil
- Decrease of air density with height.

In addition, Neubauer assumed the major constituent of the Martian atmosphere to be nitrogen rather than the recently accepted carbon dioxide. Thus, Neubauer's analysis should be updated to reflect the latest generally accepted values. It is suggested that the above improvements to the theory be made and that they be tested against terrestrial small-scale cyclones and against subsequent laboratory simulations.

A facility to simulate terrestrial and Martian small-scale cyclonic disturbances (dust devils) would be considerably different from the conventional low-speed wind tunnels used to create horizontal wind velocities. The maximum

velocities to be attained at the top of the facility would be in the range of 10 to 60 m/sec or possibly higher, depending on the grain (particle) diameter and density of the flow medium (ref. 2-20). The mass flow rate of the facility will be small relative to the facility simulating horizontal winds. A conceptual design of such a facility is shown in Figures 2-8 and 2-9.

The facility would be constructed with its flow channel mounted in a vertical position to allow the natural and induced convection to create the required flow patterns. The heat required to warm the base of the facility (simulating the soil surface) could be provided by resistance heaters located in the base, or by quartz lamps directed at the base from above. Resistance heaters in the base would be far simpler. One method of inducing the cyclonic motion of the outer flow layer (simulating the outer perimeter of the disturbance) could be accomplished by forced convection from mass addition through a series of jets mounted to introduce the flow tangentially. In another method, the mass addition would take place through very-low-speed jets and the cyclonic motion would be created by fans (possibly of the centrifugal type) located on the outer perimeter of the facility. The latter method would be used only if the required velocities could not be attained by the tangentially mounted jets.

Parametric design studies would have to be performed to establish the size of the facility. It is hoped that the same facility used to simulate the terrestrial dust devils could be used to simulate the Martian dust devils. This may be possible, but it should be pointed out that the terrestrial simulation facility using air as a flow medium could use a large, relatively low-speed fan exhausting to the atmosphere. The Martian simulation facility would not be

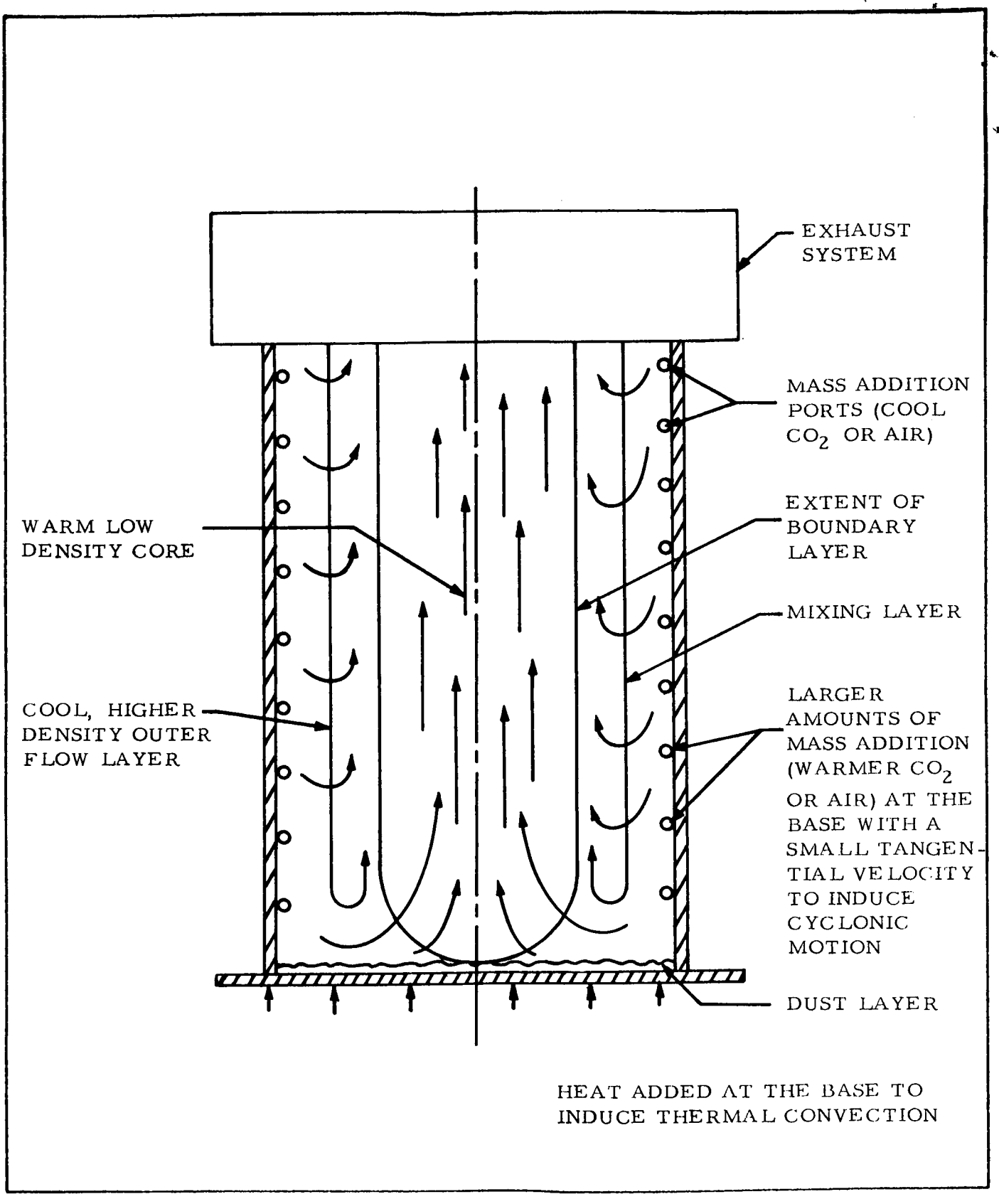

Figure 2-8. TYPICAL FACILITY FOR SIMULATION OF TERRESTRIAL AND MARTIAN DUST DEVILS

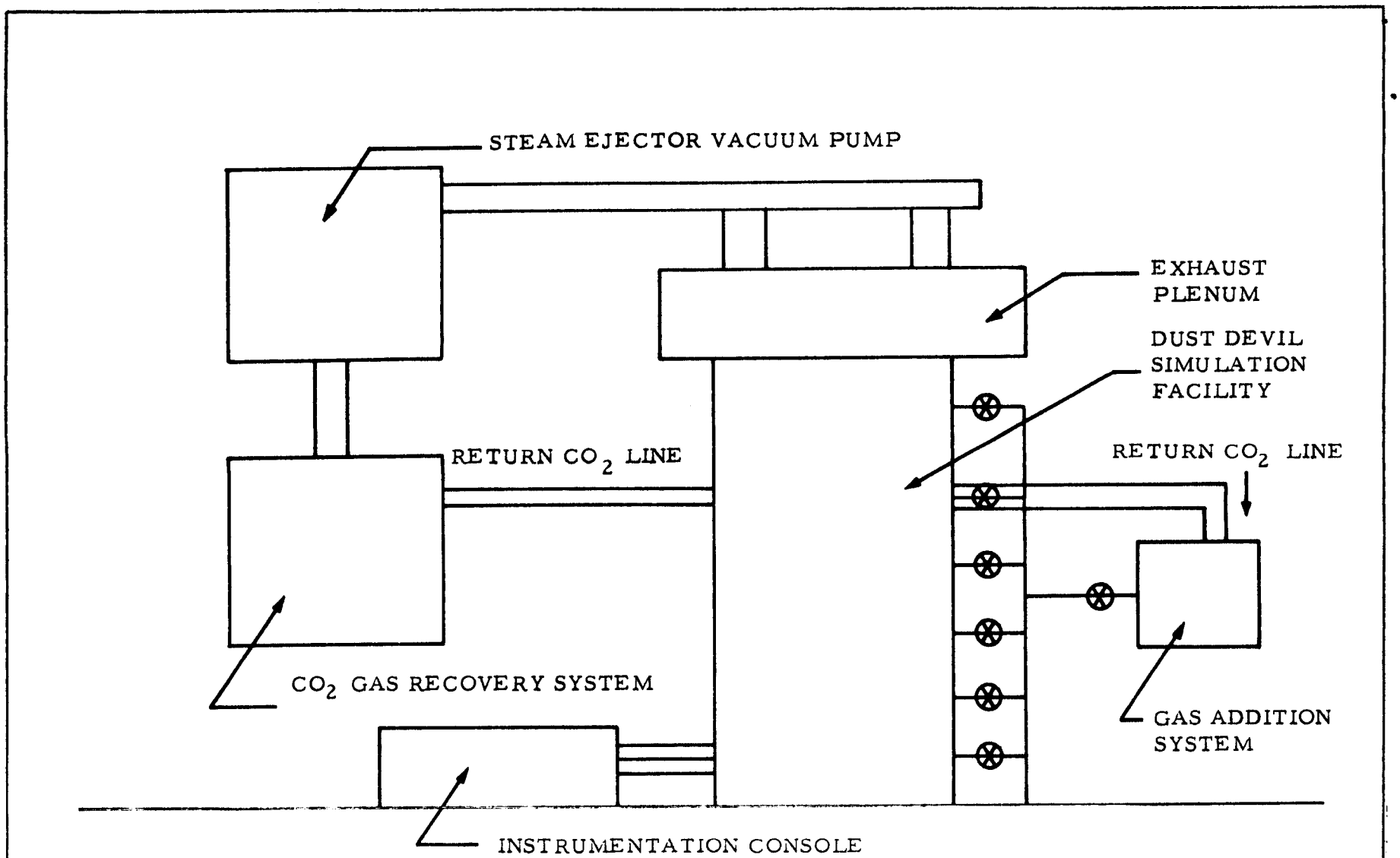

Figure 2-9. LAYOUT OF DUST DEVIL SIMULATION FACILITY

nearly as simple. Attainment of the correct static pressure would require inducing a vacuum to the level of approximately 5 to 7 mb by means of steam ejectors or similar pumps. In addition, an economical means of reclaiming the flow of gaseous carbon dioxide may be necessary. The low static pressure of the Martian facility would require much heavier construction than would the facility for terrestrial simulation.

Several of the major difficulties in simulating the terrestrial and Martian dust devils are listed and discussed as follows:

1. Attainment of Cyclonic Motion - Analytical prediction of the cyclonic motion may be very difficult. However, use of data obtained from observed terrestrial dust devils should aid facility design.
2. Inability to Simulate the Reduced Gravity of Mars - Experimental data obtained in the simulation facilities must be corrected for the reduced gravity of Mars using suitable scaling parameters (such as the Grashof number). This will reduce the effectiveness of direct observations, but should not greatly affect the validity of the results.
3. Inability to Adequately Simulate the Temperature and Pressure Profiles on Mars - This problem can be overcome in part by using forced convection thus creating at least a small pressure and temperature gradient.
4. The Martian Dust Devil Simulator Will Require Heavy Construction - This problem is also true of the Martian horizontal wind simulation facility. The construction of such a facility would require close adherence to the ASME code for unfired pressure vessels. However, construction requirements of this facility will be no more severe than for any large altitude chamber.

2.5 REFERENCES

2-1. Bagnold, R. A., The Physics of Blown Sand and Desert Dunes, Methuen and Co., Ltd, London, 1965.

2-2. Krumbein, W. D.,"Setting Velocity and Flume-Behavior of Nonspherical Particles," Am. Geophys. Union, Trans., 1942.

2-3. Krumbein, W. C., and Pettijohn, F. J., Manual of Sedimentary Petrography, Appleton-Century Co., Inc., New York, 1938.

2-4. Blair, J. T., Lucas, W. C., Stanley, J. T., and Tatom, F. B., "Analytical Model of the Martian Surface," Nortronics-Huntsville, TR-793-7-142, 1967.

2-5. Dollfus, A.,"Visual and Photographic Studies of the Planets at the Pic du Midi," Planets and Satellites, B. M. Middlehurst, University of Chicago Press, 1961.

2-6. Johnson, R. W., "Terrain and Soil of Mars," Ninth Annual American Astronautical Society Meeting, Los Angeles, California, 1963.

2-7. Ryan, J. A., "Notes on the Martian Yellow Clouds," Journal of Geophysical Research, Vol. 69, No. 18, September 1964.

2-8. JPL Technical Memorandum No. 33-234, 1966.

2-9. Weidner, D. K., and Hasseltine, C. L., ed., "Natural Environment Design Criteria Guidelines for MSFC Voyager Spacecraft for Mars 1973 Mission," NASA TM X-53616, 1967.

2-10. Opik, E. J., "The Martian Surface," Science, Vol. 153, No. 3733, 15 July 1966.

2-11. Tang, W., "Some Aspects of the Atmospheric Circulation on Mars," NASA Contractor Report, NASA CR-262, July 1965.

2-12. Neubauer, F. M., "Thermal Convection in the Martian Atmosphere," Journal of Geological Research, Vol. 71, No. 10, 15 May 1966.

2-13. Ives, R. L., "Behavior of Dust Devils," Bull. Am. Meteorol. Soc., Vol. 28, 1947.

2-14. Sinclair, P. S., "Some Preliminary Dust Devil Measurements," Monthly Weather Review, Vol. 92, No. 8, August 1964.

2-15. de Vaucouleurs, G., Physics of the Planet Mars, Faben and Faben, Ltd., London, 1954.

2-16. Kuo, H. L.,"Dynamics of Convective Vortices and Eye Formation", The Atmosphere and the Sea in Motion, The Rockefeller Institute Press (New York) in Association with Oxford University Press, 1959.

2-17. Sharp, R. P., "Wind Ripples," Journal Geology, Vol. 71, 1963.

2-18. Finkel, H. J., "The Barchans of Southern Peru," Journal Geology, Vol. 67, 1959.

2-19. Hertzler, R. B., Wang, E. S. J., Welbers, O. J., "Development of a Martian Environmental Simulation Facility," McDonnell Aircraft Corporation, St. Louis, Missouri, 1966.

2-20. Anderson, A. D., "Spherical Particle Terminal Velocities in the Martian Daytime Atmosphere From 0 to 50 Kilometers," Lockheed Palo Alto Research Laboratory, Palo Alto, California, LMSC 6-76-66-21, September 1966.

2.6 BIBLIOGRAPHY

Bell, H. S., "Density Currents as Agents for Transporting Sediments," Jour. Geol., Vol. 50, 1942.

Ford, E. F., "The Transport of Sand by Wind, Transactions, American Geophysical Union, Vol. 38, No. 2, April 1957.

Frenkiel, F. N. and Sheppard, P. A., (ed), "Atmospheric Diffusion and Air Pollution," Adv. in Geophysics, Vol. 6, New York Academic Press, 1959.

Hjulstrom, F., "Transportation of Detritus by Running Water," Recent marine sediments, Am. Assoc. Petrol. Geol., Tulsa, Oklahoma, 1939.

Nevin, C., "Competency of Moving Water to Transport Debris," Geol. Soc. Am., Bull., Vol. 57, 1946.

Pettijohn, F. J., "Weathering," Chapter 12, "Transportation, Abrasion, and Selective Sorting," Chapter 13, Sedimentary Rocks, Harper & Brothers, New York.

Reichie, P., "A Survey of a Hypersonic Jet on a Dusty Surface," Presented at the first Annual Meeting of the Institute of the Aerospace Sciences, January 1963.

Roberts, Leonard. "The Interaction of a Rocket Exhaust with the Lunar Surface," presented at a Specialist's Meeting on "The Fluid Dynamic Aspects of Space Flight, Marseille, France, 20-24 April 1964.

Russell, R. D., "Effects of Transportation on Sedimentary Particles," Recent marine sediments, Am. Assoc. Petrol. Geol., Tulsa, Oklahoma, 1939.

Scheidigger, A. E., Theoretical Geomorphology, Prentice-Hall, Inc., N. J., 1961.

Sharp, R. P., "Kelso Dunes, Mojave Desert, California," Geological Society of America Bulletin, Vol. 77, October 1966.

Thornbury, W. D., Principles of Leomorphology, John Wiley and Sons, Inc., New York, 1954.

vonKarman, T., "Sand Ripples in the Desert," Technion Yearbook, 1947.

SECTION III

DISSOCIATION AND ABSORPTION OF MOLECULAR CONSTITUENTS OF THE MARTIAN ATMOSPHERE

3.1 SOLAR RADIATIONS ATOP THE MARTIAN ATMOSPHERE

Solar radiation is the principal source of energy input to the Martian atmosphere. The solar electromagnetic radiation is expected to have the same spectral distribution at the top of the Martian atmosphere as at the top of the Earth's atmosphere since the spectral character of this radiation does not change in traveling from the Sun to any of the planets. However, due to Mars being farther from the Sun than Earth, the solar electromagnetic radiation intensity reaching Mars averages only 43 percent of that reaching the Earth. Absorption of this radiation by the gases in the upper atmosphere produces dissociation, excitation, ionization, and other aeronomical processes. The main cause of these processes is absorption of extreme ultraviolet (XUV) radiation. Corpuscular radiations do not play a significant role in the Earth's aeronomy since the Earth's magnetic field deflects most of these away; however, due to the weakness of the Martian magnetic field, corpuscular radiations may penetrate deeply into the Martian atmosphere and undergo absorption, thus affecting the aeronomy of Mars. Relevant properties of the solar electromagnetic and corpuscular radiations are summarized below.

The solar XUV radiation flux for wavelengths from 1775Å to 1Å, incident on the top of the Earth's atmosphere, have been tabulated by Hinteregger et al. (ref. 3-1). The tabulation is in terms of total flux in spectrum intervals of 50Å, except around emission lines, vs total and ionization cross sections of O, O_2, and N_2, for radiation in each interval. From 1300Å to 250Å, measurements

were made with a photoelectric scanning monochrometer employing a diffraction grating at grazing incidence. Quiet solar conditions are represented and errors are estimated at less than 30 percent. Data between 310Å to 56Å are based on a rocket experiment, and are probably correct within a factor of 2 above 150Å; but could be off as much as a factor of 3-5 toward shorter wavelengths. The data below 55Å were obtained through the work of Friedman (ref. 3-2) and Tousey (ref. 3-3) in x-ray photometry. All flux data listed are corrected for the absorption of the atmosphere gas except for those wavelengths where absorption is known to be negligible.

This represents the best present knowledge of the distribution of solar XUV radiation. Considerable effort is being expended in improving it and results can be expected apace. These results, of course, pertain directly to the case of Mars since the intensity of radiation varies according to the inverse square law and the distribution remains unchanged as one passes from Earth to Mars.

Corpuscular radiation consists of galactic cosmic radiations and solar cosmic radiations. In the case of galactic cosmic radiations, 85 percent are protons, 14 percent are alpha particles, and about 1 percent are nuclei of elements from Li to Fe. The integrated yearly flux is $\sim 7 \times 10^7$ protons/cm^2 with energy range from 40 Mev to 10^{13} Mev (predominant range 10^3 - 10^7 Mev). In the solar cosmic radiation, there are protons and alpha particles. The integrated yearly flux is 3×10^9 protons/cm^2 with energy around 30 Mev and $\sim 5 \times 10^8$ protons/cm^2 with energy around 100 Mev (ref. 3-4).

3.2 CONSTITUENTS OF THE MARTIAN ATMOSPHERE

3.2.1 Spectroscopic Findings

The existence and abundance of carbon dioxide has been well established by ground-based spectroscopic and interferometric measurements. Table 3-1 gives the measurements by various investigators (ref. 3-5). The spectral lines used by the investigators listed in Table 3-1 were the very weak rotational band at 8689Å and the medium strength rotational band at 10,488Å; both are weak-line spectra. Since the equivalent width of the line for a weak absorption band is proportional to the total abundance of the absorbing medium, this measurement gives the total abundance and the partial pressure of the carbon dioxide in the Martian atmosphere.

The Martian surface pressure estimates are based on the total pressure broadening of the carbon dioxide vibrational spectrum bands. The absorption spectrum bands result from the absorption of light at frequencies which excite transitions from one molecular vibration energy state of CO_2 to one of a higher energy. The degree of saturation of a single line and the equivalent width of a band are determined by the total effective pressure.

The equivalent width of a single line will vary in one of the following ways: (a) linearly with the effective pressure for weak lines in the band, (b) as the square root of the pressure for strong unsaturated lines, or (c) become independent of the pressure as saturation becomes complete. Measurements on CO_2 strong absorption lines made by G. Kuiper in 1962 and 1963 (ref. 3-6) give minimum and maximum pressures and abundances based on his measurements of the 1.57 and 1.6 micron lines. These measurements gave minimum and maximum surface pressures of 4.2 mb and 6.7 mb, respectively; for abundance the results were a minimum of 57 m-atm and a maximum of 90 m-atm.

In addition, isotopic absorption band spectra of $C^{13}O_2^{16}$ and $C^{12}O^{16}O^{18}$ have been observed (ref. 3-6); thus the isotopes C^{13} and O^{18} are present in addition to the more abundant isotopes C^{12} and O^{16}.

A number of deliberate attempts have been made to detect water-vapor, nitrogen, and argon through spectroscopic methods or balloon observations. Although not all such experiments were successful, some results worth noting have been obtained (Table 3-2). Since nitrogen and argon do not have strong absorption lines in the infrared region, these spectroscopic measurements do not indicate whether or not they are present.

Table 3-1. TOTAL CO_2 ABUNDANCE ESTIMATES
(ground-based spectroscopic data, weak-line spectra)

Investigators	CO_2 band	CO_2 abundance at STP(w) for $\bar{T}_{Mars} = 200°K$ m-atm.
Kaplan, Munch & Spinrad (1963) (ref. 3-8)	8,689Å	55 ± 20
Spinrad & Schorn (ref. 3-9) (1965 opposition)	8,689Å	90 ± 27
Owen (ref. 3-10) (1965 opposition)	8,689Å 10,488Å	65 ± 20
Hunten & Belton (ref. 3-11) (1965 opposition)	10,488Å	68 ± 20

*P_{CO_2} = 0.074 w mb/m/atm

Table 3-2. WATER CONTENT IN THE MARTIAN ATMOSPHERE (refs. 6, 7)

Observer(s)	Year	Water-Vapor Content	Remarks
Weaver	1963	<40μ	from a balloon
Dollfus	1963-4	150μ	narrow-band filter photometry
Spinrad, Munch & Kaplan	1963	(14±7)μ	Mt. Wilson 100-inch coude spectrograph

The following are gases which, although not detected, can conceivably be present in the Martian atmosphere: CO, CH_4, NH_3, H_2S, N_2O, NO, $COCl_2$, HCHO, COS, NO_2, etc. The upper limit values are as follows (ref. 3-4).

CO	<1 cm-atm, STP (in a vertical column on Mars)	
CH_4	<0.04 cm-atm	
NH_3	<0.01 cm-atm	
N_2O	<0.08 cm-atm	
NO	<20 cm-atm	(tests of questionable sensitivity)
H_2S	<7.5 cm-atm	
$COCl_2$	not available	
HCHO	<0.3 cm-atm	
COS	<0.2 cm-atm	
NO_2	<8 μ -atm	
H_2O	<1. cm-atm	
O_3	<0.05 cm-atm	
SO_2	<0.003 cm-atm	

Because telluric O_2 lines are quite strong and broad, making the detection of any weak Martian components very difficult with photographic techniques, molecular O_2 has not been observed. An upper limit to the Martian O_2 content of $\leq$70 cm-atm has been set by the analysis of Kaplan et al. (ref. 3-8).

3.2.2 Achievements of Mariner IV Occultation Experiments

The occultation made by the Mariner IV flyby of Mars on 15 July 1965 has greatly expanded our knowledge of Mars and its atmosphere. The highlights of the event and its findings are given in Table 3-3.

The electron density profiles above the Martian surface derived from the occultation experiment have been made by several authors. Figure 3-1 was made by Fjeldbo et al. (ref. 3-16) based on the JPL occultation team immersion model of Martian atmosphere described in Table 3-3.

Other important findings were as follows:

Mass of Mars, $GM_s/GM_m = 3{,}088{,}000$ (ref. 3-18)

Gravitational Constant, $GM_m = 42977.8\ km^3/sec^2$ (ref. 3-18)

Static magnetic field is 0.001 times that of Earth (ref. 3-18).

Based on the present knowledge of the Martian environment, three models for Martian atmosphere have been developed by MSFC, NASA, based on the assumptions of hydrostatic equilibrium and a perfect gas law among the thermodynamic quantities. The models, called "mean", "minimum", and "maximum", are each generated from a given temperature profile, molecular weight profile, and surface pressure. The appropriate details are given in reference 3-18.

3.3 AERONOMIC PROCESSES IN THE MARTIAN UPPER ATMOSPHERE

The dissociation, excitation, and ionization produced by the absorption

Table 3-3. OBSERVED DATA FROM IMMERSION AND EMERSION OF OCCULTATION (refs. 3-12, 3-13, and 3-14)

	Immersion	Emersion
Location	Electris/Mar Chronium 50.5°S, 177°E	Mare Acidalium 60°N, 34°W
Time (local)	1300, later winter	0030, later summer
Solar zenith angle, X	67°	104°
Surface refractivity[1] (N)	3.6 ± 0.2	4.2 ± 0.3
Surface scale height[2], km	9 ± 1	12 ± 1
Radius[3], km	3384 ± 3	3379 ± 4
Ionospheric characteristics: Maximum electron density	at $02^h31^m/1.2^s$GMT	at $03^h25^m9.5^s$GMT
Ionosphere[4], el/cm^3	$(9.0 \pm 1.0)\times10^4$	$<4 \times 10^3$
Altitude of maximum, km	123 ± 3	----
Electron scale height[5] above maximum, km	22 ± 3	----
Temperature	<200°K at 100-200 km	

1. Average for U.S., ~313 N (ref. 3-15).

2. Average for U.S., ~7 km (ref. 3-15). The scale heights observed on Mars show no obvious change with altitude up to 30 km.

3. From the mass center of Mars.

4. Maximum electron density at $\chi = 0°$, 1.5×10^5 el/cm^3 total electron contents at $\chi = 67°$, 5×10^{11} electrons/cm^2. Total electron content at $\chi = 0°$, 7×10^{11} electrons/cm^2. Maximum electron density for Earth at $\chi = 0°$ is 10^6 el/cm^3; and total electron content at $\chi = 0°$ is 10^{13} electrons/cm^2 (ref. 3-14).

5. Appears to be independent of altitude to approximately 250 km.

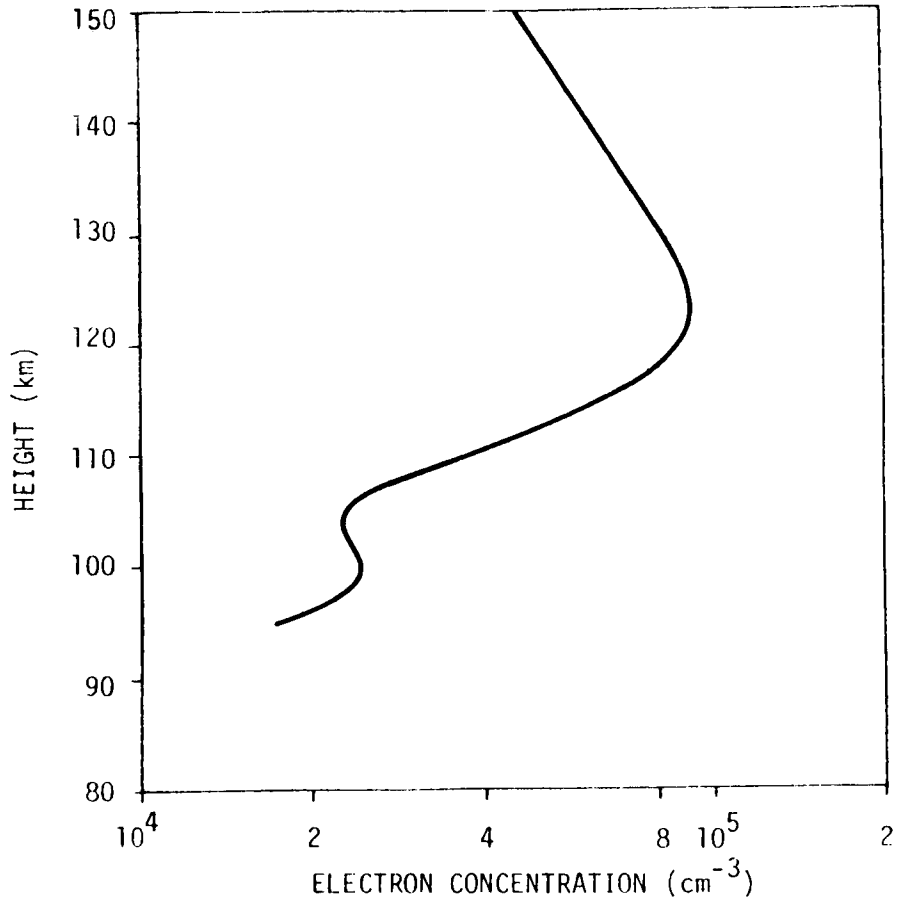

Figure 3-1. ELECTRON CONCENTRATION VS. ALTITUDE IN MARTIAN ATMOSPHERE

of solar radiation by the Martian atmosphere results in various kinds of recombination processes among the constituents. Such aeronomical processes characterize the Martian upper atmosphere and ionosphere. The study of the Martian atmosphere and ionosphere is necessarily based upon the limited knowledge gained from Mars space probes and Earth-based spectroscopic measurements; models of the Martian atmosphere then are constructed by extrapolation and analogy from our understanding of the Earth's atmosphere.

Chamberlain (ref. 3-19) has discussed the layers of Martian atmosphere in which the principal events happen. Starting from the surface and proceeding upward, we have the troposphere, mesosphere (same as for the Earth), layer of vibrational relaxation, CO_2 dissociation, (photochemical equilibrium in a layer 70 to 80 km above the Martian surface, ref. 3-16), ionosphere (with peak at 123 ± 3 km and electron density ($9.0 \pm 1.0 \times 10^4$ electrons/cm^3), and finally outer space.

3.3.1 Dissociation of Martian Upper Atmosphere by Solar Schumann-Runge Continuum

The dissociation of Martian atmospheric components is caused primarily by the Schumann-Runge continuum of solar XUV radiation (1350-1750Å) and takes place at the bottom of the ionosphere. N_2, a possible atmospheric constituent of Mars, is inactive in this respect because of its low dissociation cross section ($<10^{-22}$ cm^2). CO_2, on the other hand, has a maximum cross section of 4.4×10^{19} cm^2 at 1495Å, absorbing XUV radiation from 1690Å to 1250Å, to dissociate into CO and O. The CO and O can recombine by three-body collision to form CO_2, but a pair of O atoms can combine to form O_2. The reaction rate of the latter process is 10^3 times larger than that of the former. The relative amounts of the two molecules will be commensurate with these reaction rates.

Further, O_2 dissociates into O atoms by the absorption of XUV radiation of a wavelength range extending nearly over that of the radiation absorbed by CO_2. The maximum dissociation cross section of O_2 is 1.85×10^{-17} cm^2 at 1450Å. This is about 40 times larger than that of CO_2, and, therefore, the ultraviolet radiation may be absorbed mainly by the reaction product O_2, effectively shielding the CO_2 from dissociation. Other chemicals can be neglected because of their large activation energies. N_2 and other photochemically inactive species may take part in the processes only as third bodies (ref. 3-7). Then the reactions in the Martian upper atmosphere, denoting the third body by Z_1 (it may be CO_2, CO, O, or N_2), are as follows:

$$CO_2 + h\nu \rightarrow CO + O \qquad \text{(Dissociation)}$$

$$CO + O + Z_i \rightarrow CO_2 + Z_i \qquad \text{(Association)}$$

$$O_2 + h\nu \rightarrow O + O \qquad \text{(Dissociation)}$$

$$O + O + Z_i \rightarrow O_2 + Z_i \qquad \text{(Association).}$$

All this amounts to a qualitative description of the phenomena to be expected in the Martian upper atmosphere. In order to put it into quantitative, mathematical terms, one turns to the work of Shimizu (ref. 3-7). Assuming photochemical equilibrium and neglecting the diffusion, the equations governing the gas densities are:

$$\gamma_1[CO_2] = [CO][O] \sum_i \alpha_{1i}[Z_i] \qquad (1)$$

$$\gamma_2[O_2] = [O]^2 \sum_i \alpha_{2i}[Z_i] \qquad (2)$$

where $[\,]$ means the density of each species and γ_j is the function of height defined by

$$\gamma_j = \int J_h(\lambda)\sigma_j(\lambda)d\lambda \qquad (j=1,2).$$

$J_h(\lambda)$ is the intensity of solar XUV radiation at height h, and the quantities σ_1 and σ_2 are the dissociation cross sections of CO_2 and O_2, respectively. The dependence of σ_1 on the wavelength is quite similar to that of σ_2. The quantities α_{1i} and α_{2i} are the third-body recombination rates corresponding to the association equations above. The relative yields obtained experimentally are

$$\alpha_{O_2} : \alpha_{CO_2} : \alpha_{N_2} : \alpha_{CO} : \alpha_O = 1.0 : \quad 1.0 : \quad 0.6 : \quad 0.6 : \quad 0.1 \qquad (3)$$

The neglect of the gas diffusion gives the subsidiary conditions

$$\frac{\beta}{1-\beta}[N_2] = [CO_2] + [CO]$$

$$= [CO]/_2 + [O]/_2 + [CO_2] + [O_2] \qquad (4)$$

where β is the ratio of the concentration of CO_2 to that of the total gas before irradiation.

The dissociation of the Martian upper atmosphere may then be determined by calculating the absorption of the XUV radiation downward, and solving equations (1) through (4) at every altitude by an iterative method with the possible change of parameters. Results of such calculations performed by Shimizu (ref. 3-7) are given in Table 3-4.

Table 3-4. CALCULATED VALUES OF DISSOCIATION LAYERS OF MARTIAN ATMOSPHERE

Model	T(°K)	P(mb)	CO_2%	H(km)	Height of dissoc. layer above surface (km)	Amount of CO (cm STP)
Mariner IV	170	6	50	10	105	0.3
KMS (standard) (ref. 3-8)	160	25	16	12.4	155	0.2
KMS (low)	160	10	60	12.4	125	0.3

The calculated value obtained for CO content is 0.2 ~ 0.3 cm STP. However, observations made by Kuiper on the vibration-rotational overtone band of this molecule at 2.35μ give the upper limit as 1 cm STP. A more recently observed result by Moros, as referenced by Shimizu (ref. 3-7) gives it as 1.5 cm STP. Both are larger than the computed value.

3.3.2 Ionic Properties of the Martian Ionosphere

The spectroscopic findings combined with the Mariner IV occultation experiment indicate that the lower atmosphere of Mars may be mostly CO_2. Some investigators also claimed to have observed the H_2O absorption lines. CO_2 may not be the only gas on Mars; other gases such as nitrogen and argon may be present in significant quantities. These particular gases have not been shown experimentally to exist on Mars, but rather were chosen by analogy with their presence in the terrestrial atmosphere.

Because of the dissociation just discussed, the CO_2 in the lower atmosphere will inevitably associate with O, O_2, CO_2, CO, and C in the upper atmosphere, at and above the altitude where the photochemistry of CO_2 is important. Further,

if N_2 and A are present in the lower atmosphere they, as well as N and NO, must also be present in the upper atmosphere, although the concentrations of N, C, and NO will certainly be orders of magnitude smaller than the major constituents.

The production of ions in the Martian ionosphere can be generalized as follows: The initial production of ion-electron pairs by solar ultra-violet and x-ray radiation results in ions corresponding to each of the neutral species. Some of these ions interact chemically with neutral atoms and molecules to form new ions. Molecular ions eventually recombine with electrons to form neutral molecules (refs. 3-20 and 3-21). For example, in the Earth's atmosphere, N_2, by the absorption of radiation of 798Å, produces N_2^+ and e^-. The N_2^+ thus produced may react upon collision with N, O_2, or O to produce N_2 and N^+, N_2 and O_2^+, or N_2 and O^+. Atomic oxygen (O^+) ions are not only produced by solar radiation, but also chemically when N_2^+ collides and exchanges charge with a neutral oxygen atom. Molecular oxygen ions (O_2^+) are produced by two chemical processes in addition to production by direct photoionization. Reacting with molecular nitrogen (O^+), produces NO^+, a major ionospheric ion. The processes can be visualized easily from Figure 3-2, which shows the ionic reactions of nitrogen and oxygen, generally recognized as important in the terrestrial ionosphere.

The ionization potentials and their corresponding photon wavelengths of possible Martian atmospheric constituents are given in Table 3-5. It can be seen from the table that the ionization potentials for possible Martian atmospheric constituents are high. The ionizing radiations have shorter wavelengths than those in the Schumann-Runge continuum. The absorption cross sections and ionization cross sections of O, O_2, and N_2 are given in reference

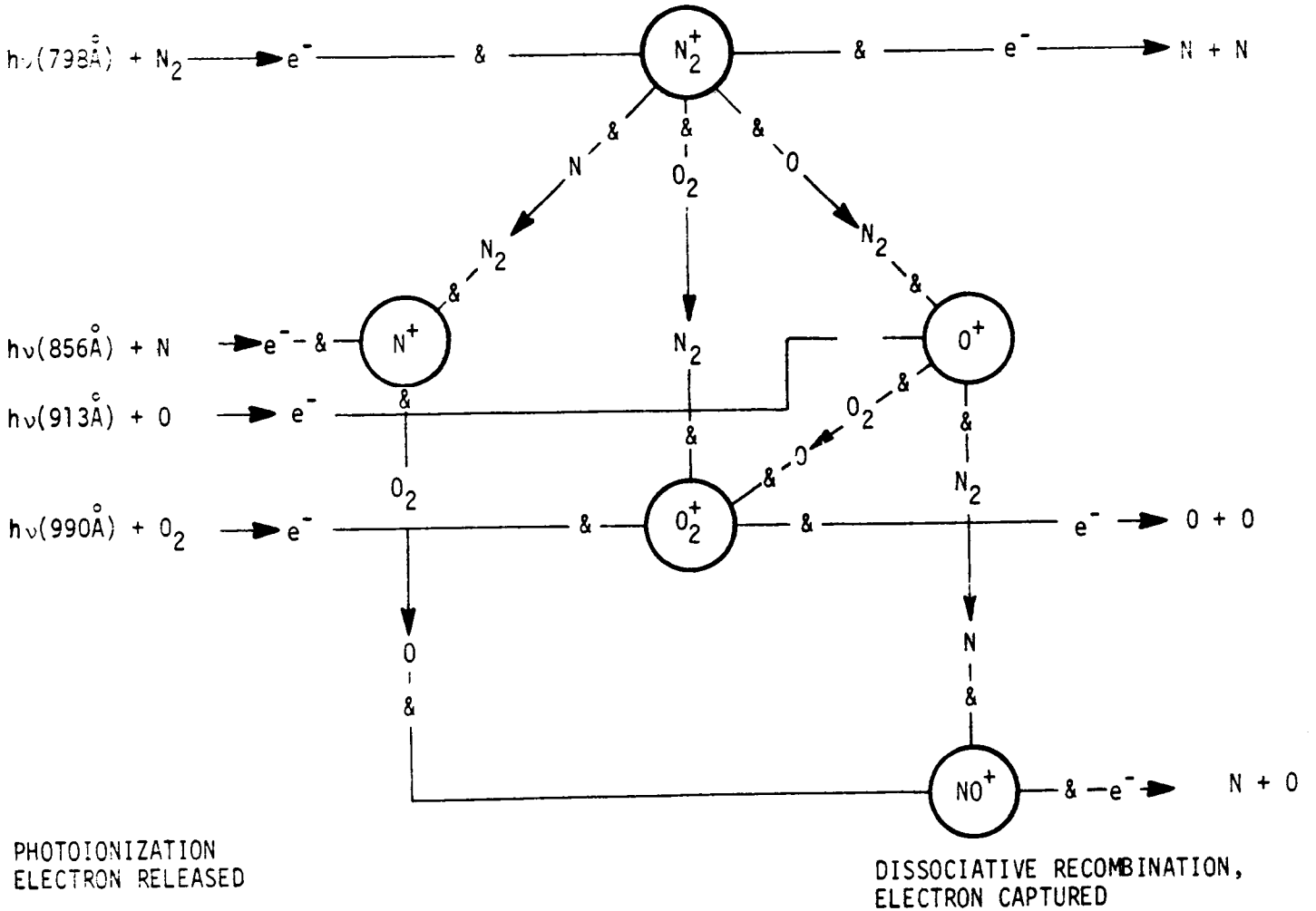

Figure 3-2. IONIC REACTIONS OF NITROGEN AND OXYGEN GENERALLY RECOGNIZED AS IMPORTANT IN THE TERRESTRIAL IONOSPHERE (3-22)

Table 3-5. THE IONIZATION POTENTIALS AND THEIR CORRESPONDING PHOTON WAVELENGTHS OF POSSIBLE MARTIAN ATMOSPHERE CONSTITUENTS (ref. 3-23)

Constituent	Ionization potential (ev) and corresponding photon λ(Å)				
	I	II	III	IV	V
CO_2	14.4(861)				
A	15.68(790)	27.76(445)	40.75(303)	61(203)	78(158.5)
N_2	15.51(798)				
N	14.48(856)	29.47(420)	47.40(271)	77(161)	97.4(127)
NO	9.5(1305)				
NO_2	11.0(1124)				
N_2O	12.9(959)				
NH_3	11.2(1104)				
H_2O	12.56(985)				
O_2	12.5(990)				
O	13.55(913)				
CO	14.1(877)				
C	11.22(1102)	24.27(510)	47.65(266)	64.22(192.7)	390.1(31.7)
CN	14(833)				
CH_4	14.5(853)				

I, II, III, IV, V are degrees of ionization.

3-1. Absorption cross sections and coefficients of the other species in the table can be found in reference 3-22.

As discussed in the preceding section, dissociation of CO_2 produces appreciable amounts of O, O_2, and CO in the upper atmosphere of Mars, while dissociation of N_2 into N is minimal. At ionospheric heights, the atmosphere is so rarefied that diffusion becomes the fastest process of molecule transport. From consideration of the resultant diffusive separation, the atomic oxygen should become the principal constituent because it is lighter than CO, N_2, O_2, Ar, and CO_2 (ref. 3-16).

Atomic oxygen is ionized by electromagnetic radiation in the wavelength interval 911-1027Å (Hinteregger group I), O^+ then becoming the principal ions in the Martian main ionospheric layer. Thus, the reaction

$$O + h\nu \rightarrow O^+ + e$$

is considered to be the most important for electron production in that layer.

There are many other electron-producing reactions, although they are not as important to the ionization of atomic oxygen. Typical examples of the reactions are the following (ref. 3-24).

$CO_2 + h\nu \rightarrow CO_2^{+*} + e$	(molecular ionization, product in excited state)
$CO_2 + h\nu \rightarrow CO^+ + O + e$	(dissociative ionization)
$CO_2 + h\nu \rightarrow CO^*$ $CO^+ + e$	(with preionization)
Compton scattering with soft x-rays	
$O^- + h\nu \rightarrow O + e$	(photodetachment)
$O_2^- + O_2 \rightarrow O_2 + O_2 + e$	(collision-type detachment)

In attempting to determine the mechanisms of electron loss, one does well to begin with consideration of processes involving the major constituents. O^+ is the principal ion in the Martian ionosphere, so a possible electron removing process is the radiative recombination of O^+ with an electron:

$$O^+ + e \rightarrow O + h\nu \quad .$$

However, it has been shown that the rate coefficient of this process is thousands of times smaller than that of the possible processes of molecular ion recombination with electrons. The direct recombination process therefore makes a very minor contribution to the total electron loss rate. The recombination of electron - O^+ pairs instead takes place in a two-step process; atomic oxygen ions (O^+) first undergo reactions with the resultant production of molecular oxygen ions (O_2^+) which in turn combine with electrons

$$O_2^+ + e \rightarrow O_2 \quad .$$

Production of O_2^+ ions from O^+ ions is effected through the following processes:

$$O^+ + CO_2 \rightarrow O_2^+ + CO \qquad k_1 \simeq 10^{-9} \text{ cm}^3/\text{sec}$$

$$O^+ + O_2 \rightarrow O_2^+ + O \qquad k_2 \simeq 10^{-11} \text{ cm}^3/\text{sec}$$

$$O^+ + N_2 \rightarrow NO^+ + N \qquad k_3 \simeq 10^{-12} \text{ cm}^3/\text{sec}$$

The first equation of this group is the most important.

The loss of electrons will therefore be dominated by the dissociative recombination of molecular ions with electrons. These are the reactions given on the right side of Figure 3-2. Recombination could also occur through the

attachment of electrons to certain neutral species. Such attachment could be collisional in nature, in which the energy of attachment is carried off as kinetic and internal energy of the final-state particles; or radiative, in which the energy of attachment is carried off as a photon. Examples of these are:

$$e + O_2 \rightarrow (O_2^-)^* \rightarrow O^- + O \qquad \text{(dissociative attachment)},$$

or

$$(O_2^-)^* + O_2 \rightarrow O_2^- + (O_2) \quad ,$$

or

$$e + CO_2 \rightarrow CO_2^- + h\nu \qquad \text{(radiative attachment)}.$$

As to the ion-neutral reactions, Norton (ref. 3-25) has listed eleven more reactions which might be important in the Martian ionosphere as shown in Table 3-6.

Table 3-6. ION-NEUTRAL REACTIONS APPROPRIATE TO MARTIAN IONOSPHERE

Reactions	Rate Coefficients at 300°K (cm^3 sec^{-1})
(1) $A^+ + CO_2 \rightarrow A + CO_2^+$	7.4×10^{-10}
(2) $A^+ + CO \rightarrow A + CO^+$	8×10^{-11}
(3) $A^+ + N_2 \rightarrow A + N_2^+$	$\geq 6 \times 10^{-12}$
(4) $A^+ + O_2 \rightarrow A + O_2^+$	1.1×10^{-10}
(5) $N_2^+ + CO_2 \rightarrow N_2 + CO_2^+$	8×10^{-10}
(6) $N_2^+ + O_2 \rightarrow N_2 + O_2^+$	1×10^{-10}
(7) $N_2^+ + O \rightarrow N + NO^+$	2.5×10^{-10}
(8) $CO^+ + CO_2 \rightarrow CO + CO_2^+$	1.1×10^{-9}
(9) $CO^+ + O_2 \rightarrow CO + O_2^+$	2×10^{-10}
(10) $C^+ + CO_2 \rightarrow CO + CO^+$	1.8×10^{-9}
(11) $C^+ + O_2 \rightarrow O + CO^+$	1.1×10^{-9}

These ion-neutral reactions have, indirectly, a very important bearing on ionospheric relaxation in that they control relative concentrations of the various ionic species by "shuffling" them as rapidly as they are formed. The nature of the ionic species has an important bearing on the rate of electron recombination and, hence, to electron density profile.

Ion-ion recombinations are also of interest in the ionsophere. They are basically of two types: two-body and three-body. Typical examples of two-body recombinations are:

$$N_2^+ + O_2^- \rightarrow N_2^* + O_2^*$$

$$O_2^+ + O_2^- \rightarrow O_2^* + O_2^{**}$$

$$O_2^+ + O_2^- \rightarrow O + O + O_2^* \quad \text{(ion-ion dissociative recombination).}$$

An example of three-body recombination is

$$N_2^+ + O_2^- + Z_i \rightarrow N_2^* + O_2^{**} + Z_i \ ,$$

where Z_i is designated for any unspecified third body.

The altitude distribution of the different constituents will be determined by their diffusion rates and by the competition of the various processes mentioned. Although an exact description cannot be made, a general understanding has been reached as a result of the occultation experiment.

In summary, the principal constituent of the Martian atmosphere in its entirety is CO_2. This dissociates into CO and O at the 70- to 80-km layer above the Martian surface. The CO_2, CO, and O will distribute in the upper

atmosphere by diffusion. O, being the lightest, will occupy a higher altitude and become the principal constituent of that particular region. Through the ionization processes, an upper layer with O^+ as the principal ion is formed. The O^+ loss processes are radiative recombination and various ion-neutral reactions. Calculations based on equilibrium conditions together with the temperature value of 80°K and a neutral scale height of 12 km yield an atomic oxygen number density of approximately 10^9 cm^{-3} at 120 km (ref. 3-17).

3.3.3 Solar Corpuscular Flux

In the quest for further information, an approach could be made in the following way (ref. 3-7). If the atmosphere is isothermal and a one-component system, the penetration depth, h, and the ionization rates of ionizing radiation and charged particles, q, may be estimated as follows. For solar fluxes

$$n(h)\,\sigma H \sim 1 \quad ,$$

$$q \sim I_\infty\,\sigma n \quad ,$$

where n(h) is the atmospheric density at the height h, σ is the ionization cross section, H is the scale height, and I_∞ the intensity of radiation at the top of the atmosphere. For radiation

$$n(h)\,\frac{dE}{dx}\,H \sim E_o \quad ,$$

and for charged particles

$$q \sim n\,\frac{F_\infty(dE/dx)}{W} \quad ,$$

where dE/dx is the energy loss of the flux per unit distance passed through the atmosphere, E_o the initial energy of the particles, F_∞ the particle flux, and W the energy necessary to make an ion pair. The calculation indicates that the effect of the solar corpuscular flux is not negligible compared with the solar XUV radiation in ionizing the atmosphere.

3.4 SIMULATION STUDY OF MARTIAN ATMOSPHERIC COMPOSITION

Our knowledge of the composition of the Martian atmosphere obtained from ground-based observations has been derived primarily from spectrograms taken of Mars. Interpretation of the spectrograms was guided by our understanding of their analogy with spectrograms of the terrestrial atmosphere and comparison with laboratory simulation experiments. The essence of the laboratory simulation experiments is to make an artificial Martian atmosphere, produce its absorption spectrum, and compare this spectrum with that actually taken of Mars. The constituents of the artificial Martian atmosphere are placed in an absorption tube with a solar (or selected) radiation source at one end and an infrared spectrograph at the other. By varying the constituents of the artificial Martian atmosphere, as well as its physical conditions (temperature, pressure, and path length), a variety of spectrograms can be obtained. Comparison of those spectrograms with those actually taken of Mars will show how close the artificial Martian atmosphere is to the real one. In earlier laboratory work, absorption tubes of high pressure (up to 50 atm) and long path (up to 45 meters) were used. However, because of the high pressure broadening of the spectral lines, a reliable gas content could not be obtained (ref. 3-26).

The success of the art of simulation, as we have seen, depends primarily on our ability to create an artificial Martian atmosphere which is as close as possible to the real Martian atmosphere.

The first consideration is that the observed Martian spectra are a blend of a solar, telluric, and Martian absorptions. The simulation of these spectra would best be made by channeling natural sunlight, received through the Earth's atmosphere, through the absorption tube that simulates the Martian atmosphere, although one cannot reproduce in this way the apparent radial velocity of the planet (ref. 3-27).

Secondly, the artificial Martian atmosphere in the absorption tube is made up so that the composition, pressure, temperature, and path length are sufficiently close to the actual Martian atmosphere and at its observed conditions. The composition and temperature of the mixture will be chosen from a given Martian atmosphere model. The partial pressure of each constituent times the path length is its abundance, and is chosen from observed data.

The gas pressure in the absorption tube, to achieve simulation, must be consistent with the pressure exerted by a unit column of such gas mixture transferred to the surface of the planet. The appropriate relation is furnished by the Curtis-Godson approximation, which states that the mean pressure along the absorbing path in a planetary atmosphere is equal to one-half the surface pressure (ref. 3-28). Thus, for example, with a CO_2 abundance of 55 m-atm and a maximum surface pressure of 5.2 mb, the CO_2 pressure in the absorption tube is 2.6 mb and the required path length, ℓ, of the absorption tube will be

$$\ell = \frac{55}{5.2/2/1000} = 21{,}200 \text{ meters.}$$

This path length is typical of the requirement for simulation. This did not seem feasible until 1942, when J. U. White (ref. 3-29) developed a

multiple-reflection-type absorption tube which could provide, in a reasonably short tube, an absorbing path comparable to the solar spectrum in the Martian atmosphere. An absorption tube used in the Yerkes Observatory, University of Chicago, is depicted in Figure 3-3. In this apparatus, there are three spherical, concave mirrors of equal radius of curvature. Two of these, A and B, are cut from one circular mirror, as shown in Figure 3-3b, and are mounted at one end of the tube; the third, C, shaped as indicated in Figure 3-3c, is mounted at the other end at a distance equal to the radius of curvature. Light from an automobile headlight bulb, or, for ultraviolet work, light from a hydrogen discharge tube, is focused on an entrance slit at 0 in Figure 3-3a and 3-3c. From there, the light falls on the two mirrors, A and B, which form images of the slit at 1 and -1, respectively, the latter being discarded. The mirror C is so adjusted that the light from A received at 1 is reflected to B. With proper adjustment, A is imaged on B, and no light is lost except for reflection losses. The mirror B then forms an image of 1 at 2, whereupon the light is reflected to A, and so on, until the light emerges at 8 after having traversed the space between the mirrors sixteen times. By turning mirror A, small increments about an axis perpendicular to the plane of the paper in Figure 3-3a, the number of images on mirror C can be readily changed. Using this system with a small glass tube 5 cm in diameter with mirrors of 150-cm radius of curvature, we can obtain a path length of 60 meters. With a metal pipe 10 inches in diameter and mirrors of 22-meters radius of curvature, a path length of 5500 meters can be obtained. The limit to the number of traversals is set by the reflection losses and by the number of images that can be accommodated on mirror C. If the latter presents no difficulty, the number of traversals through the tube that can

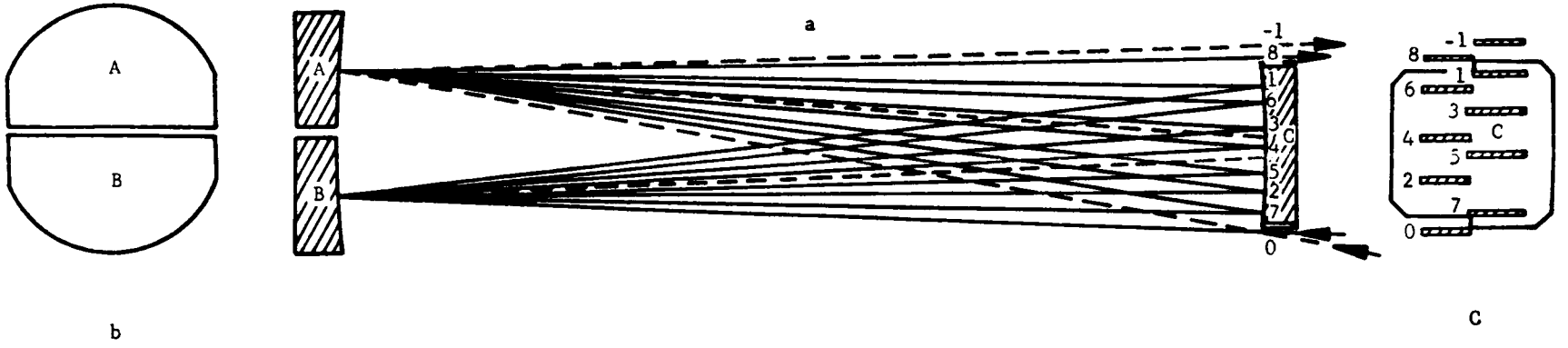

Figure 3-3. OPTICAL ARRANGEMENT FOR ABSORPTION TUBE, YERKES OBSERVATORY

be made without decreasing the efficiency of the system can be calculated from the formula

$$R^n = \frac{1}{e} \quad ,$$

where R is the reflectivity of the mirror, n is the number of traversals, and e is the base of natural logarithms (ref. 3-30).

Figure 3-4 shows such a long-path gas absorption tube attached to a spectrometer for obtaining infrared absorption spectrum (ref. 3-31).

The main function of the windows ℓ_1 and ℓ_2 is to provide a vacuum and pressure seal. Of necessity, the material must be infrared transmitting (generally KBr or NaCl). All mirrors within the tube are prealigned optically and bonded to metal mounting posts. The A and B mirrors are prealigned to the principal optical plane of C and bonded to metal posts with provisions for a push-pull rotational adjustment by screws. Focal adjustment is obtained by movement of the assembly holding A and B. The mirrors M_3 and M_5 are integral to a sub-base, which is kinematically mounted to the main base of the tube and thus can be readily removed. This allows a frequent measure of the radiation without the tube and will permit clearance to the polarizing attachment and sample tubes of other types.

This technique has been used by Herzberg (ref. 3-26) and Kuiper et al. (ref. 3-27).

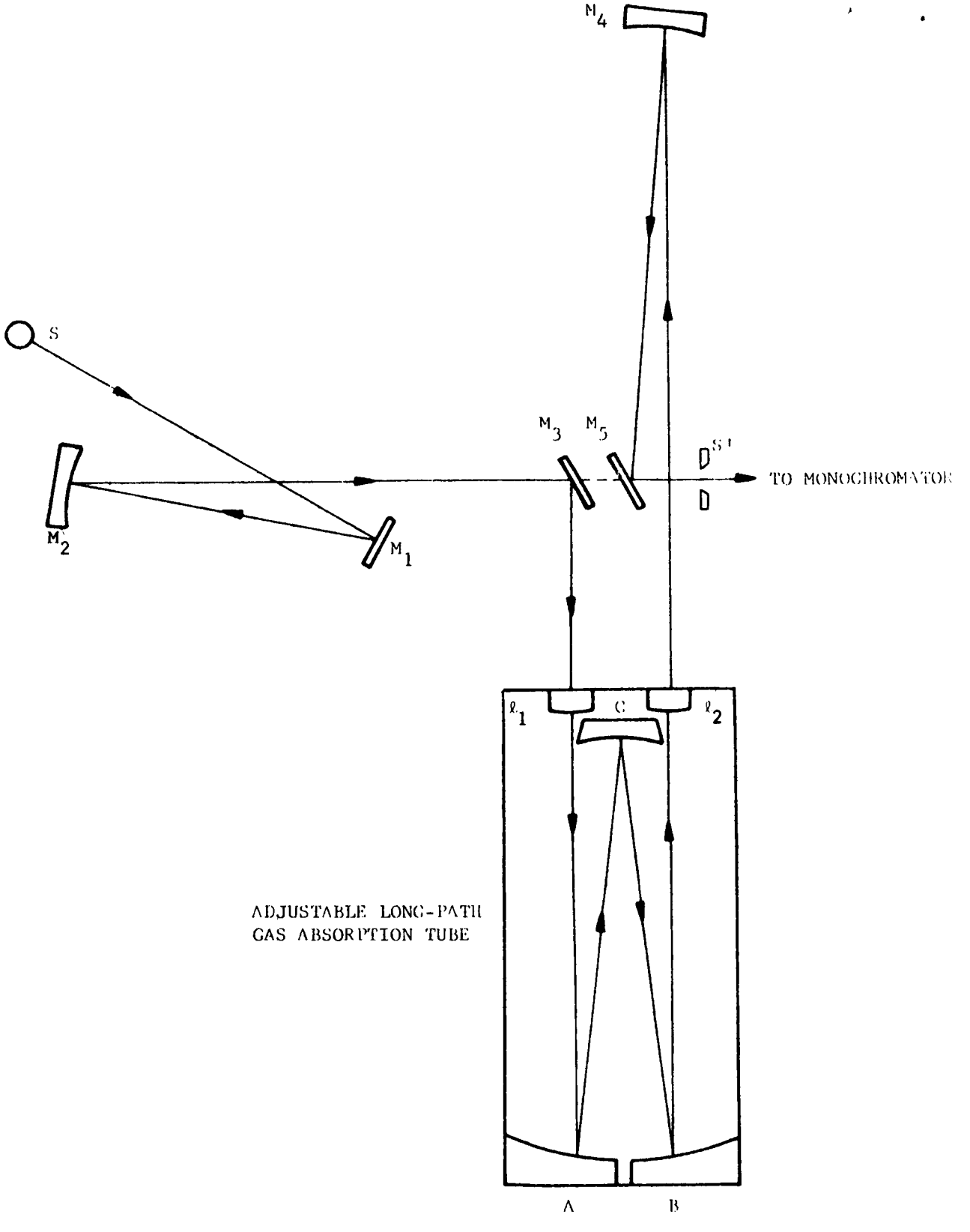

Figure 3-4. A LONG-PATH GAS ABSORPTION TUBE INSTALLED FOR OBTAINING INFRARED ABSORPTION SPECTRUM

3.5 REFERENCES

3-1. Hinteregger, H. E., Hall, L. A., Schmidtke, G., "Solar XUV Radiation and Neutral Particle Distribution in July 1963 Thermosphere," Space Research, Ed. by King Hele, D. G., Muller, P., and Righini, G., North-Holland Publishing Company, Amsterdam, 1965, p. 1175.

3-2. Friedman, H., "Rocket Spectroscopy," Space Science, Chapter 14, Ed. by Legalley, D. P., John Wiley and Sons, Inc., 1963.

3-3. Tousey, R., "The Extreme Ultraviolet Spectrum of the Sun," Space Science Review, 1963, pp. 3-69.

3-4. Owen, T. C., and Kuiper, G. P., "A Determination of the Composition and Surface Pressure of the Martian Atmosphere," Communications of Lunar and Planetary Laboratory, Vol. 2, No. 35, The University of Arizona, 1964.

3-5. Spencer, D. F., "Our Present Knowledge of the Martian Atmosphere," AIAA/AAS Stepping Stone to Mars Meeting, Am. Inst. of Aero. and Ast., New York, March 1966, pp. 532-541.

3-6. Kuiper, G. P., "Infrared Spectra of Stars and Planets, IV: The Spectrum of Mars, 1-2.5 Microns, and the Structure of its Atmosphere," Communications of the Lunar and Planetary Laboratory, Vol. 2, No. 31, The University of Arizona, 1964.

3-7. Shimizu, M., "The Atomic and Molecular Processes in the Upper Atmospheres of Planets," Rept. Ionospheric Space Res., Japan, Vol. 20, No. 3, September, 1966, pp. 271-288.

3-8. Kaplan, L. D., Munch, G., and Spinrad, H., "An Analysis of Spectrum of Mars," The Astrophys. Jour., Vol. 139, No. 1, January 1964, pp. 1-15.

3-9. Spinrad, H., Schorn, R. A., Moore, R., Giver, L. P., and Smith, H. J., "High Dispersion Spectroscopic Observations of Mars, I. The CO_2 Content and Surface Pressure," The Astrophys. Jour., Vol. 146, No. 2, November 1966, pp. 257-270.

3-10. Owen, T., "The Composition and Surface Pressure of the Martian Atmosphere: Results from the 1965 Opposition," The Astrophys. Jour., Vol. 146, No. 1, October 1966, pp. 257-270.

3-11. Hunten, D., and Belton, M., "The Abundance and Temperature of CO_2 in the Martian Atmosphere," Astrophys. Jour., Vol. 145, August 1966, pp. 454-467.

3-12. Kliore, A., Cain, D. L., and Levy, G. S., "Radio Occultation Measurement of the Martian Atmosphere over Two Regions by the Mariner IV Space Probe," Moon and Planets, Ed. by Dollfus, A., North-Holland Publishing Co., Amsterdam, 1967.

3-13. Fjeldbo, G., Fjeldbo, W. C., and Eshleman, V.R., "Atmosphere of Mars, Mariner IV Models Compared," Science, Vol. 153, No. 23, September 1966, pp. 1518-1523.

3-14. Kliore, A., Eshleman, V. R., and Drake, F. D., "Occultation Experiment, Results of the First Direct Measurement of Mars' Atmosphere and Ionosphere," Science, Vol. 149, 10 September 1965, pp. 1243-1245.

3-15. Bean, B. R., and Dutton, E. J., Radio Meteorology, National Bureau of Standards, Monograph 92, 1966.

3-16. Fjeldbo, G., Fjeldbo, W. C., and Eshleman, V. R., "Models for the Atmosphere of Mars based on the Mariner IV Occultation Experiment," Journal of Geophysical Res., Vol. 71, 1966.

3-17. Nicks, O. W., "A Review of the Mariner IV Results," Moon and Planets, Ed. by Dollfus, A., North-Holland Publishing Co., Amsterdam, 1967.

3-18. Weidner, D. K., and Hasseltine, C. L., "Natural Environment Design Criteria Guidelines for MSFC Voyager Spacecraft for Mars 1973 Mission," NASA TMX-53616, Marshall Space Flight Center, Huntsville, Alabama, June 1967.

3-19. Chamberlain, J. W., "Upper Atmospheres on the Planets," Astrophysical Journal, Vol. 136, No. 2, 1962, pp. 582-593.

3-20. Nicolet, M., and Swider, W., Jr., "Ionospheric Chemistry," Planetary Space Science, Vol. 11, 1963, p. 1459.

3-21. Holmes, J. C., Johnson, C. Y., and Young, J. M., "Ionospheric Chemistry," Space Research V, Ed. by King Hele, D. G., Muller, P., Righini, G., 1965, pp. 756-766.

3-22. Schultz, E. D., Holland, A. C., and Marmo, F. F., "Planetary Aeronomy VIII. A Congeries of Absorption Cross Sections for Wavelengths less than 3000Å," NASA CR-15, Geophysics Corporation of America, Mass., NASA, Washington, D.C., September 1963.

3-23. Handbook of Chemistry and Physics, Chemical Rubber Publishing Company, Cleveland, Ohio, 1966.

3-24. Whitten, R. C., Poppoff, I. G., Physics of Lower Ionosphere, Prentice-Hall, Inc., New Jersey, 1965.

3-25. Norton, R. B., Ferguson, E. E., Fehsenfeld, F. C., and Schmeltekopf, A. L., "Ion-Neutral Reactions in the Martian Ionosphere," Planet Space Science, Vol. 14, 1966, pp. 969-978.

3-26. Herzberg, G., "Laboratory Absorption Spectra Obtained with Long Path," The Atmosphere of the Earth and Planets, Ed. by Kuiper, G. P., Chapter XIII, University of Chicago Press, 1952.

3-27. Kuiper, G. P., "Infrared Spectra of Stars and Planets, IV: The Spectrum of Mars, 1-2.5 Microns, and the Structure of its Atmosphere, Communications of the Lunar and Planetary Laboratory, Vol. 2. No. 31, The University of Arizona, 1964.

3-28. Owen, T. C., and Kuiper, G. P., "A Determination of the Composition and Surface Pressure of the Martian Atmosphere," Communications of the Lunar and Planetary Laboratory, Vol. 2, No. 32, The University of Arizona, 1964.

3-29. White, J. U., "Long Optical Path of Large Aperture," Journal of Opt. Soc. of America, Vol. 32, May 1942.

3-30. Skymanski, H. A., and Alport, N. L., IR Theory and Practice of Infrared Spectroscopy, Plenum Press, New York, 1964.

3-31. Pilston, R. G., and White, J. U., "A Long Path Gas Absorption Cell," Journal of Optical Society of America, Vol. 44, No. 7, July 1954.

SECTION IV
THERMODYNAMIC PROPERTIES OF THE MARTIAN ATMOSPHERE

This section summarizes the results of a review of the current knowledge of the thermodynamic properties of the Martian atmosphere. The parameters discussed are those which are considered to have great importance to spacecraft design and which may lend themselves to laboratory simulation. The major objectives of this study were as follows:

- To review current knowledge of the thermodynamic properties of the Martian atmosphere.
- To identify and briefly define the significant parameters and their interrelationships.
- To suggest experiments that could be performed to clarify or augment existing knowledge of the thermal properties of the Martian atmosphere.

It is apparent that much of the information concerning the planet Mars is still basically hypothetical in nature. This lack of definitive data has led to different, even opposite, interpretations of the same observations, and often extrapolations approaching speculation. The Mariner IV data, for example, have been interpreted in several ways. The diversity of opinion and great numbers of papers based on the same data have resulted in a time-consuming literature search with minimum return. However, the need to glean factual material from the literature was recognized as an objective of this investigation, and some element of truth has been found in most material reviewed.

As shown in the following paragraphs, several thermally related parameters were selected for investigation and evaluation. Many of them relate to other technical areas also, but cannot be easily separated due to a mutual interdependence. A prime example of this, which is of particular interest to this task, is that of dissociation and ionization. These physical reactions can have a significant effect on the thermal levels and balance of the atmosphere, which, in turn, are dependent upon the atmospheric composition, altitude, energy spectrum and flux, recombination rate, etc. It is recognized that there is considerable overlap between the study of thermodynamic properties of the atmosphere and the study of dissociation and absorption.

Most of the thermodynamic experiments suggested in this section could probably be performed in the same basic facility. However, this does not hold true for all the experiments outlined in the other sections of the report. It appears that, for the feasible experiments, several different sets of basic facilities and equipment will be required. Therefore, an all-purpose Martian atmosphere simulation facility does not appear practical, either from a technical or an economic viewpoint.

4.1 RESULTS

The following list of major thermodynamic parameters and properties of the Martian atmosphere has been constructed as a guide to organizing the literature survey:

a. Surface temperature, specific heats, albedo, etc.
b. Surface to atmospheric thermal coupling.
c. Atmosphere composition.
d. Temperature versus altitude profile.
e. Density and pressure versus altitude profiles.
f. Martian winds and dust storms.

Each item on the list is quite broad and interrelated with most of the other items on the list.

Some of the most significant points concerning each of the thermodynamic parameters are listed in Table 4-1.

An excellent comprehensive survey paper of the Martian atmosphere by Brooks (ref. 4-1) has been reviewed and may be used as a quick reference for the latest information. However, Brooks' paper does not expand on the major inconsistencies and uncertainties that remain and which are of great concern in the present study. Where possible, areas that may lend themselves to experimental verification and simulation will be pointed out.

The more significant thermodynamic parameters are discussed in the following paragraphs and are also listed in Table 4-1. Although the table is self-explanatory, it represents an attempt to present the material in a simple heuristic fashion.

4.1.1 Surface Temperatures

The surface temperature refers to the temperature of the Martian "air" only a few meters above the solid lithosphere surface. This specification is necessary since it is believed (ref. 4-2) that there can be a large variation in the surface atmosphere temperature and the surface ground temperature. In fact, as a result of the radio occultation experiment of Mariner IV (ref. 4-3), the surface atmosphere temperature was deduced as approximately $180 \pm 20°K$ while the surface temperatures were suggested to be approximately 240°K for the

Table 4-1. THERMODYNAMIC PARAMETERS OF THE MARTIAN ATMOSPHERE

PARAMETER CONSIDERED	QUANTITY AND QUALITY OF CURRENT KNOWLEDGE	CURRENT HYPOTHESES REVIEWED	RELATIONSHIPS TO OTHER PARAMETERS	SIGNIFICANCE	KEY DATA REQUIRED	NUMBER AND KIND OF DIRECT MEASUREMENTS REQUIRED	SUITABILITY OF PARAMETER TO LABORATORY INVESTIGATION
(a.1) Surface Atmosphere Temperatures	Available data limited but fairly good.	Fjeldlo et al., 1966a; Anderson, 1965	Related to Scale Ht., H and mass, m: $T = Hmg/k$	Allows calculation of surface pressure. Important to studies of thermal convection	Scale height and mass density of the lower convective layers.	1. Direct temperature measurements via landing vehicles 2. Additional radio occultation experiments	POOR: Investigation of various effects inherent in occulation experiment possible thru limited simulation in laboratory
(a.2.) Surface (soil) Temperatures	Several sources Fair Data	Gifford, 1956; Sinton and Strong 1960; Opik, 1966	Related to convective heat transfer coeff., h_c, and to the thermal properties of the soil.	Surface (soil) and Surface (air) temperatures are poorly coupled thermally, but relationship can not be neglected.	Surface (soil), thermal conductivity, specific heat, reflectivity, etc.	Direct temperature measurements via landing vehicles	Can investigate physical properties of Martian soil (predicted) in laboratory
(a.3) Optical properties of the atmosphere and surface	Fair amounts of data considered to be of good quality	Opik, 1960, 1962, and 1966; Johnson, 1963; de Vaucouleurs, 1963.	Related to atmospheric heat budget.	Important to calculation of surface to atmospheric thermal coupling and vertical temperature profile.	Transmissivity, specific scattering, surface reflectivity, and integral albedo.	1. Additional earth based spectrometric and radiometric abs. 2. Direct measurements via landing and orbital vehicles	FAIR: Could investigate optical properties of relatively thin layers of the atmosphere by assuming the composition to be known.
(a.4) Thermal properties of the Martian soil	Limited amount of data but relatively good agreement.	Neubauer, 1966; Leovy, 1966	Related to vertical temperature profile near the surface.	Determines to a large extent the surface-to-atmospheric thermal coupling.	Soil density, soil thermal conductivity, soil specific heat, convective heat transfer coefficient.	1. Retrieval of Martian surface samples highly desirable.	GOOD: Thermal properties of predicted Martian surface materials can be readily determined in the laboratory.
(b.) Surface to atmosphere thermal coupling	Limited knowledge mainly conjecture	Anderson, 1965; Leovy, 1966; Neubauer, 1966.	Affects temperature profiles near surface. Tropopause height dependent on surface temperature profile	Lack of information tends to make selection of temperature lapse rates and accurate gross thermal and atm. motion patterns difficult	Surface (soil) to surface (air) temperature profiles, exact atmospheric composition, etc.	1. Direct temperature and atmospheric composition measurements via landing vehicles. 2. Additional radio occultation experiments	POOR: Would be very difficult to simulate the natural surface convective currents.

Table 4-1. THERMODYNAMIC PARAMETERS OF THE MARTIAN ATMOSPHERE (CONT'D)

PARAMETER CONSIDERED	QUANTITY AND QUALITY OF CURRENT KNOWLEDGE	CURRENT HYPOTHESES REVIEWED	RELATIONSHIPS TO OTHER PARAMETERS	SIGNIFICANCE	KEY DATA REQUIRED	NUMBER AND KIND OF DIRECT MEASUREMENTS REQUIRED	SUITABILITY OF PARAMETER TO LABORATORY INVESTIGATION
(c.) Atmospheric composition	Large amounts of data for some selected species; virtually none for others.	See Brooks (1967) for a comprehensive survey.	Related to the thermal convection near the surface and the vertical temperature and pressure profiles.	Extremely important to the heat transport mechanisms in the atmosphere, especially above the base of the ionosphere.	Species concentration of the atmosphere as a function of altitude and of time.	Direct composition and number density measurements via orbital satellites.	POOR: Simulation of the atmospheric composition of Mars is not regarded very feasible. However, see (d.) for other possibilities
(d.) Temperature versus altitude profile and temperature lapse rate(s)	Several recent sources, give good agreement at specific altitudes only. Most data from Mariner IV and spectroscopic measurements from Earth.	Anderson, 1965; Fjeldbo et al., 1966a; Roberts and West, 1966. Poor agreement on temperature profiles (Fjeldbo, 1966b)	Adiabatic lapse rate calculated from $A = g/C_p$ Related strongly to pressure and number density	Profile of atmospheric mass density much lower than that of Earth at all altitudes. Temperatures in region of ionosphere are are very cold.	Density scale height, atmospheric composition, characteristic time constant for the sublimation of CO_2, and the reaction rate coefficients for all predicted reactions and their temperature dependence	1. Direct temperature and atmospheric composition measurements via orbital and landing vehicles. 2. Direct mass and no. density measured by similar vehicles. 3. Direct solar irradiance measurements similar vehicles.	Can investigate the reaction rate coefficients for all suspected reactions and their temperature dependence. Can determine the characteristic time constant for CO_2 sublimation under various conditions of density temperature, and solar irradiance.
(e.) Density and pressure versus altitude profiles	Large number of atmospheric models. Agreement is relatively poor, especially in region above base of ionosphere. Disagreements due to different hypotheses regarding the dissociation and recombination processes taking place.	Fjeldbo et al., 1966 Prabhakara and Hogan, 1965; Chamberlain and McElroy, 1966; Johnson, 1965; Weidner and Hasseltine, 1967.	Related strongly to atmospheric composition, vertical temperature profiles, and the heat budget of the atmosphere	Important to design of orbital and landing vehicles. Requires re-evaluation of theories such as the vertical velocities required to carry dust into the atmosphere	Pressure scale height, temperature, and atmospheric composition as a function of altitude	Direct measurements of density and temperature via orbital satellites.	POOR: Laboratory simulation of the pressure and density versus altitude profiles is not regarded feasible. However, some conjecture may be removed by suggestions made in (d.)
(f.) Martian winds and dust storms	Good observations of dust clouds are available. Sources of the clouds are based mainly on conjecture.	Opik, 1966; Tang, 1965; Ryan, 1964; Neubauer, 1966.	Related to atmospheric circulation patterns, diurnal and temporal temperature variations, surface properties and vertical structure of the atmosphere.	Important to the design of landing vehicles and in the predictability of local Martian disturbances (storms).	Wind directions, velocities, and duration; particle sizes and properties	1. Additional spectrometric observations of cloud movements and formation. 2. Direct measurements of wind velocities and directions; direct observations of dust cloud formations and movement.	GOOD: Simulation of the formation of dust storms by both horizontal and cyclonic (dust devil) winds is considered feasible (see Section II of this report).

time, conditions, and location of the Mariner IV measurements (see Table 4-2). However, as discussed in the next paragraph, the surface temperature was based on radiometric observations made prior to 1956 (ref. 4-4). Therefore, it is only conjecture at this time that the temperature differential was as high as suggested. However, Gifford established that the diurnal variation of the air temperature at 2 meters above the Gobi desert (Earth) in June is only about 25 percent of that at the surface.

Although the radio occultation data of Mariner IV may be considered to have produced the most accurate temperature (and density) data to date, it represents only one data point relative to time, conditions, and geographic location. It is unfortunate that more such instrumented flights have not been made.

The surface atmosphere temperature was calculated from the equation

$$T_{atm} = H\ m\ g/k \quad ,$$

where H is the pressure scale height, m is the mean molecular mass, g is the gravitational acceleration (at Mars' surface), and k is the Boltzmann constant. The scale height (H) was measured by the Mariner IV occultation experiment and the mean molecular mass was assumed on the basis of the models given in items 4 to 7 of Table 4-2. Of course, the jusitification for the preponderance of carbon dioxide in the models is because the total surface pressure deduced from the occultation experiment is approximately the same as the partial pressure of carbon dioxide (4 to 6 mb) measured spectroscopically from Earth (refs. 4-5 and 4-6).

Table 4-2. SUMMARY OF PRELIMINARY RESULTS FOR THE LOWER ATMOSPHERE OF MARS-MARINER IV DATA

(ref. 4-3)

1. Location	Immersion was over Electris at 50 deg S. latitude, 177 deg E. longitude, local time 1 p.m., winter, solar zenith angle 67 deg.
2. Surface Refractivity	3.6 ± 0.2 N - units
3. Surface Scale Height	9 ± 1 km
4. Surface Number Density (a) All CO_2 (b) Up to 20 percent N_2 and/or Ar	 $1.9 \pm 0.1 \times 10^{17}$ mol/cm^3 $2.1 \pm 0.2 \times 10^{17}$ mol/cm^3
5. Surface Mass Density (a) All CO_2 (b) Up to 20 percent N_2 and/or Ar	 $1.43 \pm 0.10 \times 10^{-5}$ g/cm^3 $1.50 \pm 0.15 \times 10^{-5}$ g/cm^3
6. Temperature near surface (a) All CO_2 (b) Up to 20 percent N_2 and/or Ar	 180 ± 20°K 175 ± 25°K
7. Surface Pressure (a) All CO_2 (b) Up to 20 percent N_2 and/or Ar	 4.9 ± 0.8 mb 5.1 ± 1.1 mb

Knowing the surface (air) temperature and the total molecular number density, the total surface pressure may be calculated from the equation of state

$$P = nkT \quad .$$

Obviously then, the data required to measure the surface (air) temperature - other than direct measurements using landing vehicles - is the pressure scale height and the surface mass density.

Hopefully, additional instrumented flights will be made having the ability to make similar measurements from which the temperature may be deduced or, even better, measured directly.

4.1.2 Surface Ground Temperatures

This parameter was briefly discussed above in relationship to the surface atmosphere temperature. Most of the available knowledge of the surface temperature of Mars comes from radiometric observations assembled by Cifford and Sinton and Strong (ref. 4-7). Figure 4-1 (ref. 4-8) gives the diurnal temperature variation from observations taken in 1954, when the planet was near perihelion, nearest to the Sun and Earth. The values given in Figure 4-1 include tentative corrections to the data of Sinton and Strong as made by Opik (ref. 4-9) for imperfect emissivity. The dashed portion of the curve for the nocturnal temperatures represents estimations by Opik (ref 4-8), who suggests that the large diurnal temperature amplitude indicates a low thermal conductivity of the upper surface materials.

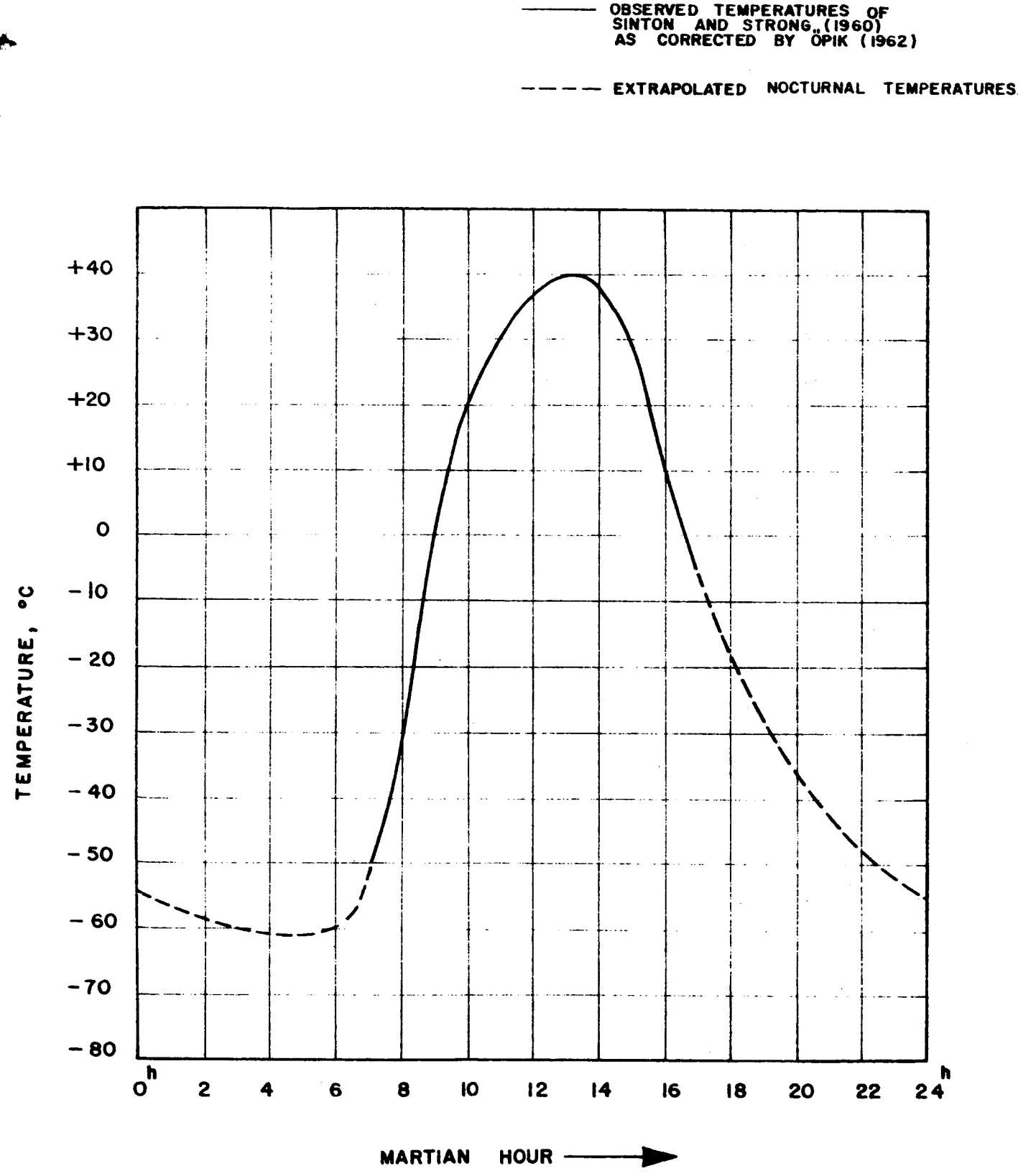

Figure 4-1. DIURNAL VARIATION OF SURFACE TEMPERATURE ON THE MARTIAN EQUATOR AT PERIHELION

The observations of Sinton and Strong support an extreme diurnal temperature variation of about 100°C at the equator. This increases considerably the diurnal variation of 50°C reported earlier by Gifford. The paper by Gifford displays some charts of seasonal temperature distributions as a function of geographic location on Mars. Although these tempratures may be considered somewhat in error now, the isotherm patterns were somewhat self-consistent and many of the patterns corresponded to well-known surface markings.

It has been postulated (ref. 4-2) that the noontime, equatorial ground-surface temperature for Mars could be 75° K higher than the air temperature near the ground, which illustrates very poor thermal coupling between the atmosphere and lithosphere. Part of this poor coupling is attributed to a very low thermal conductivity for the surface material, with a value approximating that of atmospheric air near the surface of Earth (ref. 4-8).

Values of surface thermal conductivity, specific heat, reflectivity, etc., are required to provide a basis for mathematically predicting the surface temperatures. Radiometric observations from orbital vehicles and direct temperature measurements are encouraged. Additional laboratory investigations of the thermophysical properties of possible Martian surface materials would provide more useful information concerning the composition of the lower atmosphere.

Some more recent average temperature values (Table 4-3) were reported by Johnson (ref. 4-10). These are based on observations made at the Mt. Wilson and Lowell observatories using vacuum thermocouples.

Table 4-3. SURFACE TEMPERATURE DATA FOR MARS

EVENT	TEMPERATURE (°K)
Mean temperature of illuminated disk	248
Tropical diurnal temperature	
Sunrise	225 to 215
Midday	265 to 285
Sunset	280 to 265
Polar Caps	
Average	205
Limbs	260

4.1.3 Optical Properties of the Atmosphere and Surface

4.1.3.1 Transmissivity and Specific Scattering of the Atmosphere, and Surface Reflectivity Table 4-4 provides some data on the transmission coefficient (p) and specific scattering of the Martian atmosphere (a), and the reflectivity of the surface (s). These values were compiled by Opik (refs. 4-9 and 4-11) based on Russian observations made with a small (6-inch) telescope (ref. 4-12).

Table 4-4. SOME SELECTED OPTICAL PROPERTIES OF THE MARTIAN ATMOSPHERE AND SURFACE

WAVELENGTH (Å)	p	a	s
4600 (Blue)	0.83	0.20	0.25
5200 (Green)	0.54	0.22	0.25
5430 (Green-Yellow)	0.60	0.23	0.34
5800 (Yellow)	0.69	0.24	0.40
6400 (Red)	0.74	0.20	0.53

4.1.3.2 Albedo - According to Opik (ref. 4-8), the albedo for Mars in the blue and violet range is about 0.15. Thus, only approximately 15 percent of the violet light is truly scattered in all directions, while 85 percent is absorbed and converted into heat. On the basis of a paper by Kuiper (ref. 4-13), Johnson (ref. 4-10) lists a value of 0.148 for the integrated visual albedo.

However, the acceptance of a value of 0.15 or 0.148 for the integrated albedo seems inadvisable. According to G. de Vaucouleurs (ref. 4-14), "...new data on the spectral reflectivity curve of Mars... in conjunction with the spectral energy curve of the Sun, lead to a value of 0.25 for the radiometric or integral albedo of Mars. This is significantly higher than the visual value of 0.15 often used in the past in theoretical calculations on the heat budget of the planet; hence, somewhat less solar energy, in the ratio 0.75/0.85, is available at and near the surface of Mars than we thought perviously."

The foregoing paragraph requires careful consideration since some authors are still using albedo values of 0.15 while others are using values of 0.25 to 0.26. For example, Neubauer (ref. 4-15) used a value of 0.26 for the integrated albedo in his study of the thermal properties of the Martian surface. This appears to be a serious inconsistency and is a problem area that should be resolved before any further serious studies are made of the overall heat budget.

4.1.4 Thermal Properties of the Martian Surface

Most of the following values for the thermal properties of the Martian surface are based on the assumption that the surface near the equator is a

fairly homogeneous layer of finely powdered goethite or limonite having a characteristic size of not more than a few microns. Table 4-5 is a tabulation of some of these latest derived and assumed values. The paragraphs following Table 4-5 explain the sources of the values.

Table 4-5. THE THERMAL PROPERTIES OF THE MARS SURFACE

QUANTITY	UNITS	VALUE	REPORTED BY	DERIVED OR ASSUMED PARAMETER
ρ_d (Density)	gm/cm^3	2.7	Neubauer (1966)	Assumed
ρ_d (Density)	gm/cm^3	2.0	Leovy (1966)	Assumed
$k\rho_d c$	$cal^2/sec \cdot cm^4 \cdot °K^2$	1.53×10^{-5}	Neubauer (1966)	Derived
$k\rho_d c$	$cal^2/sec \cdot cm^4 \cdot °K^2$	5.76×10^{-6}	Leovy (1966)	Derived
k (Thermal conductivity)	$cal/cm \cdot sec \cdot °K$	3.3×10^{-5}	Neubauer (1966)	Derived
k (Thermal conductivity)	$cal/cm \cdot sec \cdot °K$	2.0×10^{-5}	Leovy (1966)	Derived
c (Specific heat)	$cal/gm \cdot °K$	0.173	Neubauer (1966)	Assumed
h_c (Convective heat transfer coefficient)	$cal/cm^2 \cdot sec \cdot °K$	0.35×10^{-4} to 1.1×10^{-4}	Leovy (1966)	Derived

4.1.4.1 Density at the Surface. Johnson (ref. 4-10) reports calculations made by MacDonald (ref. 4-17) which give a mean surface density of 3.8 to 3.9 gm/cm^3 at zero depth. The later values taken by Leovy and Neubauer were based on the assumption that the Martian surface material is similar to finely powdered goethite or limonite (Table 4-5).

4.1.4.2 The Parameter ($k\rho_d c$). A value of 1.53×10^{-5} $cal^2/sec\ cm^4\ °K^2$ was calculated by Neubauer from a heat balance based on a temperature curve obtained from Planets and Satellites (ref. 4-18). The temperature curve used belonged to one of the bright areas believed to consist of goethite or limonite. Leovy calculated a value for $k\rho_d c$ of ~ 5.76×10^{-6} $cal^2/sec \cdot cm^4 \cdot °K^2$ by a similar procedure using a diurnal temperature curve from Sinton and Strong. Their temperature curve was based on observations, all of which were taken within a few latitudinal degrees of the equator.

The value of $k\rho_d c$ derived by Neubauer is larger than the value derived by Leovy by a factor of over 2. Part of this discrepancy may be due to the different values taken for the albedo (0.15 for Leovy and 0.26 for Neubauer). This was discussed earlier in the subsection on albedo. Another possible reason for the discrepancy may be due to the assumption by Neubauer that the main constituent of the Martian atmosphere is nitrogen rather than carbon dioxide. This does not invalidate the analysis of Neubauer, but the work should be updated with the latest values of pressure and composition.

4.1.4.3 Specific Heat. Neubauer obtained the value of specific heat for the surface material from an extrapolation of a table for c(T) of goethite in Landolt-Bornstein (ref. 4-19). The value taken by Neubauer was c = 0.173 cal/gm·°K. Leovy cited a value of $\rho_d c$ ~ 0.30 $cal/cm^3 °K$ which was said to be considered representative of powdery limonite, or of fine quartz sands. Leovy assumed that this product could be broken into ρ_d = 2 gm/cm^3 and c = 0.15 cal/gm°K. The source of Leovy's data was not listed.

4.1.4.4 Thermal Conductivity. The value of k = 3.3×10^{-5} cal/cm·sec·°K, as reported by Neubauer was derived from the product $k\rho_d c$ and the values for goethite and limonite. Likewise, the value of k ~ 2×10^{-5} cal/cm·sec·°K determined by Leovy was determined from the product $k\rho_d c$ as explained previously.

4.1.4.5 Convective Heat Transfer Coefficient. Leovy suggested that the order of the convective heat transfer coefficient should be $h_c \sim 10^{-4}$ cal/cm^2·sec.°K. He was able to conclude this from a heat balance where it was assumed that the linear convective heat-flux was a good approximation for forced convection with steady winds.

4.1.5 Surface to Atmosphere Thermal Coupling

The thermal coupling in question refers to how well heat is transferred from the surface to the atmosphere. From the literature reviewed thus far, it is apparent that only a very limited knowledge exists on this subject. Most conjectures appear to agree with that of Anderson who suggests that great convective instability can occur in the lowest layers of the atmosphere. As mentioned previously, the wide diurnal temperature variations and the possibly large surface-to-atmosphere temperature differentials could create unstable convective layers near the surface.

The most recent theoretical analyses reviewed concerning thermal convection near the surface of Mars are those by Leovy and Neubauer. Neubauer's paper supports the highly interesting contention that convective instability near the surface can cause small-scale cyclonic disturbances (dust devils), and that these disturbances provide an explanation for the yellow clouds that have been observed on Mars. This phenomenon was discussed in much greater detail in Section II.

Direct measurements of the temperature profiles in these lowest convective layers may be possible if performed by landing vehicles. Measurements

from orbital vehicles, i.e., the radio occultation experiment, fail due to the uncertainty of the height of specific topographical features along the limb.

The thermal coupling, as described here, is not felt to be very amenable to Earth-based laboratory simulation. However, some analytical correlation may be made by studying actual Earth environmental thermal coupling.

4.1.6 Atmospheric Composition

Details of the atmospheric composition have been covered in the comprehensive report by Brooks (ref. 4-1) which represents the most recent survey paper on the atmosphere of Mars. Although nitrogen was originally thought to be the major atmospheric constituent of Mars, it is now believed that carbon dioxide is the major constituent since it is compatible with both the Mariner IV occultation experiment and spectroscopic measurements (ref. 4-3).

Brooks summarizes the gaseous composition as follows: "...The gases and vapors can be grouped in three classes according to estimates of their abundances: (1) CO_2, A, Ne, N_2; (2) O, O_2, H_2O, CO; and (3) O_3, NO, NO_2, N_2O_4, and all others. The total abundances of the groups are of the order of magnitude of 100 m-atm, 5 cm-atm, and 5 micron-atm, or 99.95 percent, 0.05 percent and 0.000005 percent, respectively, of the total atmosphere. With considerable uncertainty, it can be stated that CO_2 accounts for about 70 percent, argon and/or neon about 20 percent, and N_2 about 10 percent, but it is realized that CO_2 may constitute more than 90 percent of the atmosphere if the total pressure is found to approach the CO_2 partial pressure."

4.1.7 Temperature Versus Altitude Profile

4.1.7.1 Temperature Versus Altitude Profile Above the Tropopause. There is general agreement among several investigators regarding important temperature points inferred and deduced from the Mariner IV radio occultation experiment. Specifically, agreement exists on a surface (atmosphere) temperature of approximately 180 $\pm$ 20°K and a temperature of approximately 80 to 85°K in the region near 100 km above the surface (refs. 4-2, 4-3, 4-20, 4-21). However, there are two major discrepancies or areas of disagreement that should be pointed out; one appears to be of considerably more consequence than the other.

First, the temperature-versus-altitude profiles below approximately 100 km are generally in poor agreement, although they all tend to follow the same trend (Fig 4-2). The region of greatest disagreement below 100 km appears to be between approximately 50 km and 90 km. The main explanation given for this disagreement (ref. 4-22) is that the exact sublimation and diffusion times for CO_2 are not completely known for this region. Fjeldbo et al. (ref. 4-22) assumed an F_2 model allowing the temperature below 100 km to dip well below the saturation temperature for CO_2. Johnson (ref. 4-23) also assumed an F_2 ionosphere model; however, he assumed that the temperature profile from the top of the convective layer (~14 km) up to about 100 km approximately follows the vapor-pressure curve for dry ice. It may be possible to perform laboratory tests to determine the relative diffusion and sublimation times for CO_2 at various temperatures and number densities.

The second and possibly most significant area of disagreement in the temperature versus altitude profiles is in the region of the ionosphere and above. The disagreement resides in identifying the main ionospheric layer

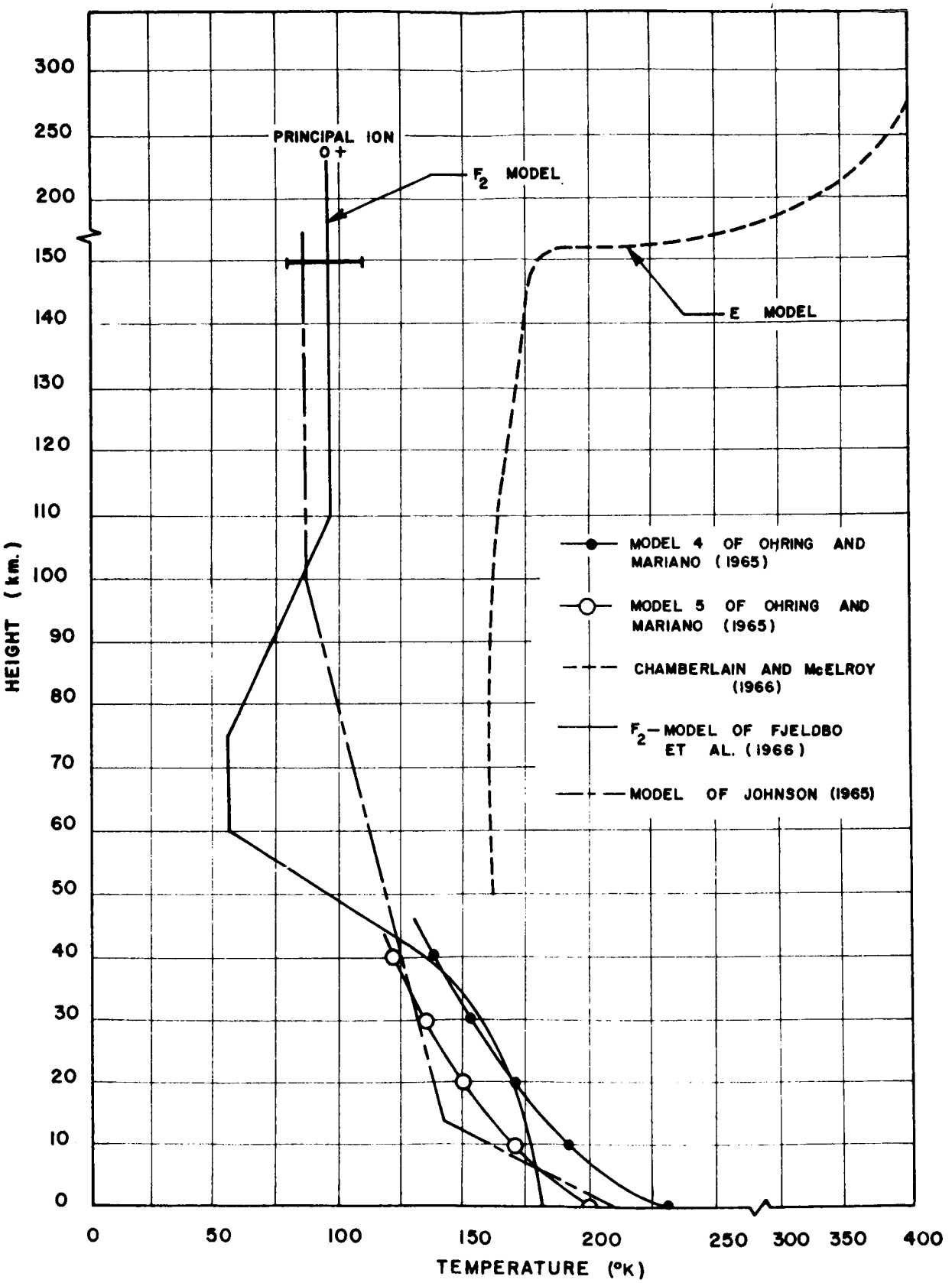

Figure 4-2. TEMPERATURE VERSUS ALTITUDE FOR SOME SELECTED ATMOSPHERIC MODELS

measured by Mariner IV as being analogous to a terrestrial F_2, F_1, or E layer. Several investigators including Johnson (ref. 4-23) and Fjeldbo et al. (ref. 4-22) have suggested an F_2 model while others support the E model. The large and very serious disagreement in the range of temperatures predicted by the two models is depicted by Figure 4-2. The details of the disagreement will not be covered here since they are well covered in the above reports. However, it should be pointed out that the ambiguous interpretations of the radio occultation data at ionospheric heights results in proposed neutral number densities differing by factors up to 10^4 and suggested upper-atmospheric temperatures varying from approximately 100°K more than 400°K (ref. 4-22). This disastrously wide range of values is not a result of design criteria parametric studies. It is a result of a variety of interpretations of the occultation experiment data.

There is a possibility that laboratory investigations of the most suitable rate coefficients may be made for gases approaching 80°K. Knowledge of the temperature dependence on the rate coefficient may help alleviate some of the uncertainties in the controlling reactions.

4.1.7.2 Adiabatic Lapse Rates to the Tropopause. Based on the results of Mariner IV, Johnson (ref. 4-23) suggested the F_2 model shown in Figure 4-1. He assumed that the fall in temperature from the surface atmosphere value to the tropopause, through the convective layer, should be adiabatic. He suggested that the temperature, through most of the atmosphere, should run along the dry-ice vapor-pressure line which sets the temperature at the tropopause altitude (14 km) at 140°K. Thus, with a surface atmosphere temperature of 210°K, the adiabatic lapse rate is about 5°K for an atmosphere assumed to consist mainly of carbon dioxide.

Models 4 and 5 of Ohring and Mariano (ref. 4-25) are in fair agreement with the model of Johnson (ref. 4-23) in the troposphere and the lower part of the atmosphere to approximately 45 km. Ohring and Mariano assumed adiabatic convective lapse rates to the tropopause, but computed the radiation temperature change rates as a function of altitude. Therefore, the temperature profiles of Ohring and Mariano do not exhibit linear adiabatic lapse rates.

The adiabatic lapse rate calculated by Anderson (ref. 4-2) for a surface atmosphere temperature of 210°K is 5.44°K/km, which is in fair agreement with the 5°K/km determined by Johnson (ref. 4-23). The adiabatic lapse rate can be determined from

$$A = g/C_p ,$$

where g is the acceleration of gravity and C_p is the mean value of the specific heat capacity at constant pressure.

4.1.8 Density and Pressure Versus Altitude Profiles

Figures 4-3 and 4-4 show comparisons of the number density and pressure versus altitude profiles for various atmospheric models. These models generally represent the effects of assuming different atmospheric compositions and making different assumptions about the heat transfer processes taking place.

The models of Weidner and Hasseltine (ref. 4-20) and Evans et al. (ref. 4-26) represent the extreme variability in the Maritan atmosphere for the design of spacecraft and should not be considered as representative of the actual Mars atmosphere. Three model atmospheres of differing atmospheric composition, surface pressure, and surface temperature were assumed by Weidner and Hasseltine (the upper density model - 48.8 percent CO_2 and 51.2 percent N_2; the mean density

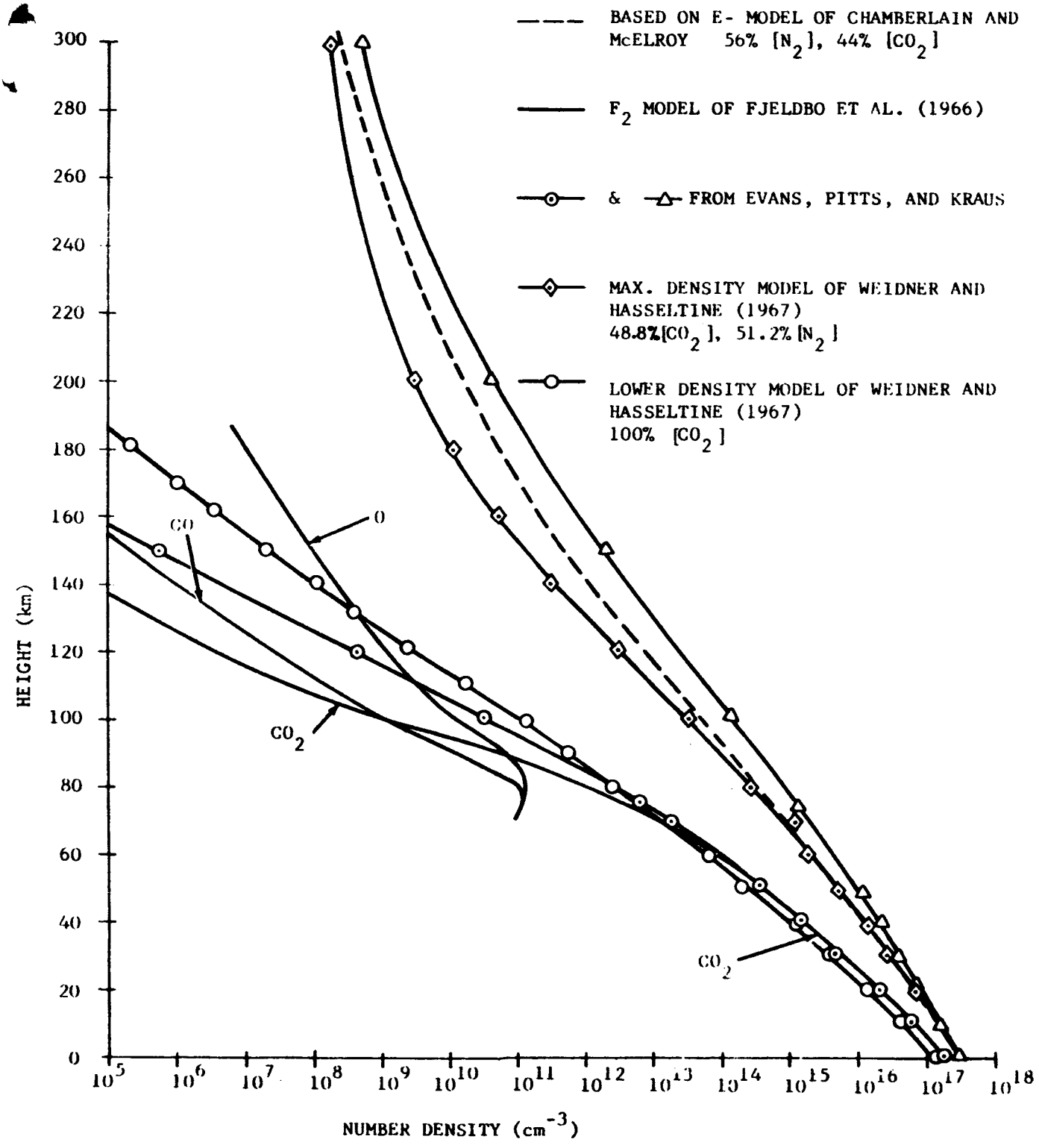

Figure 4-3. NUMBER DENSITY VERSUS ALTITUDE FOR SOME SELECTED ATMOSPHERIC MODELS

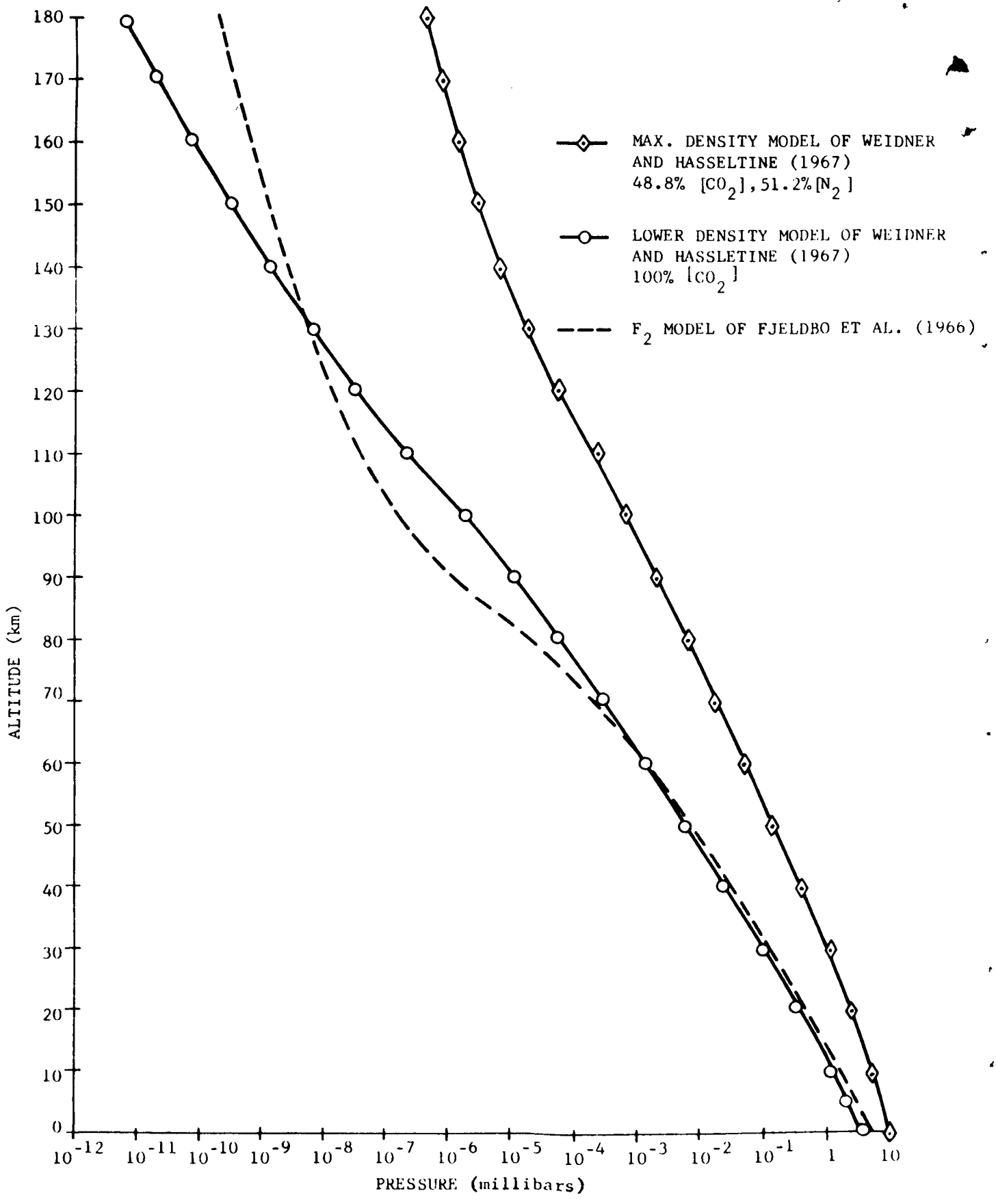

Figure 4-4. PRESSURE VERSUS ALTITUDE FOR TWO DIFFERENT INVESTIGATORS

model - 75 percent CO_2 and 25 percent N_2; and the lower density model - 100 percent CO_2). The MSFC Planetary Atmosphere Computer Program was used in generating these models). The lower density model appears to agree quite well with that of Fjeldbo et al., (ref 4-3) due to the large percentage (100) assumed for carbon dioxide. Weidner and Hasseltine assumed that the atmosphere at 60 km would change from a purely mixed medium to a gas undergoing strong dissociation and diffusive equilibrium. The assumption was made that when the carbon dioxide is dissociated, the resulting atomic oxygen and carbon monoxide begin to undergo diffusive separation.

The number density profile of Chamberlain and McElroy (ref. 4-24) is based on an available radiative model of Prabhakara and Hogan (ref. 4-27) having a surface pressure of 10 millibars and an assumed composition of 44 percent CO_2 and 56 percent N_2 (including 0.4 percent O_2). They insist that the lifetime of a CO_2 molecule against photodissociation "...is 3×10^6 seconds, or about 1 month, high in the atmosphere. But in the main dissociation region the lifetime is much longer. For example, with photochemical equilibrium ... the optical thickness to ultraviolet is 9.4 at the O_2 peak, so that here a CO_2 molecule could survive intact for 10^3 years." In addition, Chamberlain and McElroy assumed that the constituent gases were homogeneously mixed throughout the atmosphere although it was admitted that this is an oversimplification and represents the opposite extreme to models based on complete dissociation. Even when models with much lower densities and temperatures are assumed at the base of the ionosphere, the temperatures calculated for the ionospheric peak and the thermosphere are still extremely high compared to models of other investigators. In particular, Chamberlain and McElroy assumed the temperature (100°K) and density at 70 kilometers as used by Johnson (ref. 4-23)

to test the effect of lower temperatures and densities on their model. The height of 70 kilometers was chosen since Johnson suggested that the onset of diffusive separation began at this level and, also, that it was the level at which direct solar heating became of importance. Chamberlain and McElroy subsequently calculated a temperature of 285°K at 125 kilometers (in the region near the observed ionospheric peak) and an exospheric temperature of 375°K, both of which are in serious disagreement with the nearly isothermal temperature of 85°K as suggested by Johnson.

The previous paragraph concerning the large disagreement in the ionosphere and exosphere temperatures has been included here because it is tied so strongly to the assumed models of density and composition. The use of Model I of Prabhakara and Hogan in the calculations of Chamberlain and McElroy seems inconsistent with the generally accepted density and composition models of other investigators who assume that the Martian atmosphere is composed mainly of carbon dioxide (refs. 4-2, 4-3, and 4-23). The serious disagreement that exists will certainly not be resolved in this feasibility study; however, the disagreement appears to stem from the difficulty in specifying a model that is consistent with physical observation and is at the same time self-consistent with assumed dissociation, recombination, and diffusive separation models.

4.1.9 Martian Winds and Dust Storms

The feasibility of simulating the horizontal winds and small-scale cyclonic disturbances for Mars and the Earth is discussed in Section II along with a brief review of the current knowledge and related hypotheses.

4.2 POTENTIAL EXPERIMENTS

The review of present knowledge concerning the Martian atmosphere has pointed out several experiments that could aid in clarifying and explaining certain anomalies and unknowns of the atmosphere. In fact, several assumptions made concerning the Martian atmosphere are based on incomplete data from laboratory experiments performed on Earth.

In addition to the experiments listed below, some highly interesting and instructive experiments relating to thermal convection and winds near the surface of Mars (and Earth) are proposed in Section II.

4.2.1 Polarization Studies of CO_2 and H_2O Frosts

There is still a considerable amount of uncertainty concerning the composition and physical make-up of the "polar caps" and the so-called "blue haze". According to G. de Vaucouleurs (ref. 4-28), the polar caps were definitely proven to be "ice" (frozen water) by Gerard P. Kuiper. From Kuiper's direct spectrophotometer investigations, it was theorized that the polar ice caps were not thick snow and ice fields, but were only thin coverings of frost. This theory was still supported as late as 1964 (ref. 4-29).

The radio occultation experiment of Mariner IV has shown the surface pressure to be about 4 to 5 mb. This experiment, along with earlier determinations of the partial pressure of CO_2 on Mars, has substantiated the theory that CO_2 is the major constituent of the Martian atmosphere. Also, more accurate surface pressure measurements have resulted in better estimates of the surface (ground) and surface (atmosphere) temperatures. This new information has prompted the theory that the polar caps are composed mainly

of precipitated carbon dioxide with possibly a very thin film of water ice covering the solid carbon dioxide. This theory has been suggested by Leighton and Murray (ref. 4-30) who state that "...CO_2 should precipitate out and accumulate at the higher latitudes during local winter." They felt that the possibility of a thin film of the frozen H_2O at the top of the receding CO_2 polar caps might alter the "...reflective properties of the cap enough to make it appear to be composed of water ice."

Thus, a very simple experiment could be performed to investigate the nature and amount of polarized light given off by various combinations of solid carbon dioxide and water frost formed under the predicted temperature and pressure environment of the Martian polar caps. This study could not be entirely conclusive until more accurate temperature values are obtained for the regions under consideration.

Although possibly more difficult to simulate under laboratory conditions, additional polarization studies of "clouds" formed of frozen crystals of H_2O and CO_2 may shed new knowledge concerning the so-called "blue-haze" of Mars. Carbon dioxide as well as carbon and hydrocarbon smoke have been suggested by Salisbury (ref. 4-31) as possible candidates for the "blue-haze".

4.2.2 Determination of the Reaction Rate Coefficients, k_1, at Temperatures Approaching 80°K

The Mariner IV occultation experiment has provided new and highly instructive information about the Martian atmosphere. However, in establishing a definitive model for the atmosphere, a great deal of conjecture remains concerning such phenomena as the chemical reactions taking place in the upper

atmosphere and ionosphere. One such model has been formulated (ref. 4-3) based on the present information about the critically important rate coefficients for ion loss processes. The significance of this model is the choice of the critically important reaction and rate coefficient for the loss of ionized oxygen in the main ionospheric layer. Atomic oxygen was chosen to be the principal constituent above some altitude due to its lightness compared to CO, N_2, O_2, A, and CO_2. According to Fjeldbo et al., "...the most promising model (for the upper atmosphere) appears to be the one in which reaction (5) ($O^+ + CO_2 \rightarrow O_2^+ + CO$, $k_1 \cong 10^{-9}$ cm^3/sec) is the dominant rate mechanism in the main ionospheric layer." (Rate coefficient, k_1, times particle density equals loss rate). However, the rate coefficient (k_1) was taken as that measured at 300°K rather than at 80°K (the predicted ionospheric temperature), and the temperature dependence on the rate coefficient is not well known. Therefore, revisions may have to be made in this atomic oxygen-carbon dioxide model of the upper atmosphere when new information is obtained on the temperature dependence of the rate coefficients.

An intensive study should be made of the temperature dependence of the most suitable rate coefficients. This could very possibly be done in a cryogenically cooled vacuum chamber. As discussed earlier, the most important rate coefficient be to investigated is that associated with the loss of ionized atomic oxygen as depicted by the equation

$$O^+ + CO_2 \rightarrow O_2^+ + CO.$$

4.2.3 Determination of the Significant Reactive Processes in the Upper Atmosphere

In association with the experiment and disucssion presented in subsection 4.2.2, it is suggested that an investigation be made of all chemical reactions

suggested as being possible in the Martian atmosphere. According to Fjeldbo et al., the most likely possibilities appear to be:

$$O^+ + CO_2 \rightarrow O_2^+ + CO \qquad k_1 \simeq 10^{-9} \text{ cm}^3/\text{sec}$$

$$O^+ + O_2 \rightarrow O_2^+ + O \qquad k_2 \simeq 10^{-11} \text{ cm}^3/\text{sec}$$

$$O^+ + N_2 \rightarrow NO^+ + N \qquad k_3 \simeq 10^{-12} \text{ cm}^3/\text{sec} \ .$$

These and other likely chemical reactions should be investigated along with a determination of the temperature dependence of their rate coefficients.

4.2.4 Determination of the Characteristic Time Constant for CO_2 Sublimation

Fjeldbo et al. (ref. 4-22) have deduced a temperature versus altitude profile (Figure 4-2) based on the assumption that all the CO_2 in the atmosphere is supercooled. However, they suggested that this may well not be the case and some CO_2 sublimation might take place. They showed that the temperature and number density profiles may deviate widely from the supercooled case if varying amounts of sublimation are allowed. The exact amount of sublimation taking place could not be predicted since the characteristic time constant for the process is not known.

It is suggested that the relative amounts of sublimation nuclei could be determined for different degrees of supercooling in a simulation facility. Such a facility would require the ability to maintain selected vacuum pressures and temperatures while simultaneously being able to determine the degree to which the gas is supercooled. The major problems anticipated with such a study are:

- Accounting for the gas and sublimation nuclei that condense on the cool chamber walls.

- Measurement of the actual number of sublimation nuclei present per unit volume for any given condition of temperature and pressure.

It is believed that solutions to these problems can be found. For example, the mass of carbon dioxide being deposited continuously on the cooled walls of the facility may be measured by cryogenic quartz-crystal microbalances (ref. 4-32). The amount of sublimation nuclei present may possibly be measured by visualization techniques such as ultraviolet fluorescence.

4.2.5 Determination of the Convective Heat Transfer Coefficient Near the Surface of Mars

One of the most recent calculations for the convective heat transfer coefficient near the surface of Mars was made by Leovy (ref. 4-16). Leovy suggested a range for this coefficient of $\sim 0.35 \times 10^{-4}$ to $\sim 1.1 \times 10^{-4}$ cal/cm^2 sec°K. It was assumed that the linear convective heat-flux law could be expected to be a good approximation for forced convection with steady winds. The basic exchange of heat among the ground, atmosphere, and space was assumed to be expressed by

$$h(T_o - T_h) = \varepsilon\sigma T_o^4 - R_b + h_c(T_o - T_a),$$

where T_o is the Martian surface temperature, h and T_h are parameters related to radiative processes as well as to conduction and convection in the atmosphere, ε is the infrared emissivity of the ground, σ is Stefan's constant, R_b is the flux of back radiation, and h_c is a convective heat-transfer coefficient. The parameter T_a depends on the temperature distribution in the atmosphere.

In conjunction with the experimental investigation of the horizontal wind storms (Section II), it is suggested that studies of the convective heat transfer

coefficient be made in the same facility. This should pose little problem since the temperature profile above the surface of the flow facility can be measured readily at several stations. Also, measurements of the radiation arriving at the surface of the facility may be taken or estimated.

The importance of such a measurement is its relationship to the initiation of winds and dust devils through natural convection. Before performing the aforementioned convective heat-transfer tests, the proper scaling laws must be investigated for natural and forced convection under similar circumstances. This could, perhaps, result in the suggestion of smaller-scale tests that could furnish the desired information more efficiently and economically.

4.3 REFERENCES

4-1. Brooks, E. M., "Comprehensive Summary of the Available Knowledge of the Meteorology of Mars and Venus," NASA Contractor Report, NASA CR-786, May 1967.

4-2. Anderson, A. D., "A Model for the Lower Atmosphere of Mars Based on Mariner IV Occultation Data," Lockheed Palo Alto Research Laboratory, Palo Alto, California, Rept. No. 6-75-65-62, December 1965.

4-3. Fjeldbo, G., Fjeldbo, W. C., and Eshleman, V. R., "Models for the Atmosphere of Mars Based on the Mariner IV Occultation Experiment," Stanford Electronics Laboratories, SEL-66-007, January 1966 (1966a).

4-4. Gifford, F. A., Jr., "The Surface-Temperature Climate of Mars," The Astrodphysical Journal, Vol. 123, January-May, 1956, pp. 154-161.

4-5. Kaplan, L. D., Munch, G. and Spinrad, H., "An Analysis of the Spectrum of Mars," Astrophysics Journal, 139, 1964, pp. 1-15.

4-6. Kuiper, G. P., "Infrared Spectra of Stars and Planets, IV: the Spectrum of Mars, 1-2.5 Microns, and the Structure of its Atmosphere," Communication of the Lunar and Planetary Laboratory, 2, 1964, pp. 79-112.

4-7. Sinton, W. M., and Strong, J., "Radiometric Observations of Mars," Astrophysics Journal, Vol. 131, 1960, pp. 459-569.

4-8. Opik, E. J., "The Martian Surface," Science, Vol. 153, No. 3733, 1966.

4-9. Opik, E. J., Progress in the Astronautical Sciences, Vol. 1, North-Holland, Amsterdam, 1962, p. 282.

4-10. Johnson, R. W., "Terrain and Soil of Mars," Ninth Annual Meeting of the American Astronautical Society, 15-17 January 1963, p. 406.

4-11. Opik, E. J., "Journal of Geophysical Research," Vol. 65, 1960, p. 3057.

4-12. Barabashev, N. P., and Chekirda, A. T., Circ. Kharkov Observ., No. 9, 1952.

4-13. Kuiper, G. P., "The Atmosphere of the Earth and Planets," American Journal of Physics, Vol. 28, October 1960, pp. 618-622.

4-14. Vaucouleurs, G. D., "Optical Studies of the Surface and Atmosphere of Mars," In: Exploration of Mars, Advances in the Astronautical Sciences, Vol. 15, Edited by G. W. Morgenthaler, 1963, pp. 519-532.

4-15. Neubauer, F. M., "Thermal Convection in the Martian Atmosphere," Journal of Geophysical Research, Vol. 71, No. 10, 15 May 1966, pp. 2419-2426.

4-16. Leovy, C., "Note on Thermal Properties of Mars," Icarus, Vol. 5, 1966, pp. 1-6.

4-17. MacDonald, G. J. F., "On the Internal Constitution of the Inner Planets," Journal of Geophysical Research, Vol. 67, July 1962, pp. 2945-2974.

4-18. Kuiper, G. P., Ed., Planets and Satellites, University of Chicago Press, 1961, p. 434.

4-19. Landolt-Bornstein, Zahlenwerte and Funktionen ans Physik, Chemie, Astronomie, Geophysik und Technik, Vol. 3, Springer-Verlag, Berlin, Gottingen, Heidelberg, 1952.

4-20. Weidner, D. K., and Hasseltine, C. L., "Natural Environment Design Criteria Guidelines for MSFC Voyager Spacecraft for Mars 1963 Mission," NASA TMX-53616, Marshall Space Flight Center, Huntsville, Alabama, June 1967.

4-21. Kliore, A., Cain, D. L., Levy, G. S., Eshleman, V. R., Fjeldbo, G., and Drake, F. D., "Occultation Experiment: Results of the First Direct Measurement of Mar's Atmosphere and Ionosphere," Science, Vol. 149, 1965, pp. 1243-1248.

4-22. Fjeldbo, G., Fjeldbo, W. C., and Eshleman, V. R., "Atmosphere of Mars: Mariner IV Models Compared," Science, Vol. 153, No. 3743, 23 September 1966 (1966b), pp. 1518-1522.

4-23. Johnson, F. S., "Atmosphere of Mars," Science, Vol. 150, 1965, pp. 1445-1448.

4-24. Chamberlain, J. W., and McElroy, M. B., "Martian Atmosphere: The Mariner Occultation Experiment," Science, Vol. 152, No. 3718, 1 April 1966, pp. 21-25.

4-25. Ohring, G., and Mariano, J., "The Vertical Temperature Distribution in the Martian Atmosphere," Journal of Atmospheric Sciences, Vol. 23, No. 2, March 1966.

4-26. Evans, D. E., Pitts, D. E., and Kraus, G. L., "Venus and Mars Nominal Natural Environment," NASA SP-3016, 1967.

4-27. Prabhakara, C., and Hogan, J. S., "Ozone and Carbon Dioxide Heating in the Martian Atmosphere," Journal of Atmospheric Sciences, 22, March 1965, pp. 97-109.

4-28. Vaucouleurs, G. D., "Mars," Scientific American, May 1953, p. 65.

4-29. Owen, R. B., "The Martian Environment," National Aeronautics and Space Administration, NASA TMX-53167, 19 November 1964.

4-30. Leighton, R. C., and Murray, B. C., "Behavior of Carbon Dioxide and Other Volatiles on Mars," Science, Vol. 153, 8 July 1966, pp. 136-144.

4-31. Salisbury, F. B., "Martian Biology," Science, Vol. 136, No. 3510, 6 April 1962, p. 17.

4-32. Youngblood, W. W., "Capture Coefficient Determinations of Directed (Molecular Beam) and Random Fluxes of Gaseous Carbon Dioxide and Water Vapor on a Cryogenically Cooled Crystal," Northrop Space Laboratories, Huntsville, Alabama, SP-792-7-196, June 1967.

SECTION V

CONCLUSIONS AND RECOMMENDATIONS

Our knowledge of Mars is based on terrestrial observations and the Mariner IV flyby, and falls somewhat short of satisfactory design criteria. Simulation studies would increase our present knowledge and supplement the results of future terrestrial observations and space probes. This is especially true for the Martian atmosphere.

Disagreements still persist on the vertical structure of the Martian atmosphere, but even so there is now general agreement that the pressure profile remains below that of the Earth at any altitude.

The main disagreement concerning the vertical structure of the Martian atmosphere involves specification of the main ionization layer as observed by Mariner IV. Scientific and engineering requirements indicate that an answer to this disagreement must be obtained since the proposed ionosphere models vary by factors of 10^4 in number density at ionospheric heights, and upper atmosphere temperatures vary from 100° to 400°K.

Little information is available concerning wind velocities, circulation patterns, probability of sand and dust storms, and related phenomena. However, the results of this study indicate that conditions necessary for the transportation and deposition of dust or sand and the formation of characteristic landforms are present on Mars. Correct interpretation of sand and dust storms and eolian landforms could supply further information concerning Martian wind velocities, circulation patterns, and particle densities long before planetary probes penetrate the Martian lower atmosphere.

The primary objective of this study was to investigate, from a scientific and engineering design criteria standpoint, the feasibility of obtaining further Martian atmosphere information through simulation of the Martian atmosphere. Three areas studied during this study include; simulation of transportation and deposition of dust and sand by atmospheric processes, thermodynamic properties of Martian atmosphere, and dissociation and absorption properties of molecular constituents in the Martian atmosphere.

The results of these studies not only indicate that simulation studies are necessary for supplying design criteria data for future spacecraft, but also are a necessity for the accurate interpretation of data returned from early planetary probes. Earlier simulation studies, where experiments were conducted in the simulation of space, planetary, and terrestrial phenomenon, have proven to be of scientific and engineering value.

A comprehensive program composed of theoretical studies, simulation experiments, and, in some areas, terrestrial field work is necessary to ensure accurate spacecraft design data and the accurate interpretation of data returned from planetary probes. In the following paragraphs, recommendations are suggested for the implementation of such a program.

The results of the section concerning the simulations of transportation and deposition of dust and sand by atmospheric processes indicate that impact threshold velocities range from 75 m/sec to 55 m/sec. The former are calculated using a 4-mb atmospheric model and a roughness factor equivalent to a rough terrestrial desert, the latter using a 10-mb atmospheric model and a roughness factor approximately seven times as rough. While these velocities are high, they are within the range of velocities predicted for Martian surface

winds and do not unduly tax the state-of-the-art of simulation technology. The advancements in recent years of simulation technology and measuring techniques makes it possible to improve the accuracy and to expand the scope of earlier studies to include a large variety of samples (density, size, shape, etc., of particles) and environmental conditions. Three types of simulation facilities are desirable: a horizontal wind facility, a dust devil simulator, and an unconsolidated material physical properties laboratory, each with the capability of simulating both terrestrial and Martian environmental conditions. Several areas are open to further investigation; primarily, evaluating and updating previous theoretical studies for use as a guide for planning and evaluating simulation experiments and facilities, simulation of eolian processes under both terrestrial and Martian environmental conditions, supplementing these experiments with experiments concerning the physical properties of unconsolidated material, theoretical and experimental studies of electrostatic effects, and field studies to validate theoretical and experimental studies.

In the area of dissociation and absorption, it is strongly recommended that effort be directed along two phases of work: theoretical studies, and absorption tube simulation. These two phases of study are effective, simple, and ground-based. Theoretical studies of aeronomical processes of the Martian upper atmosphere should also be conducted along the same line as earlier terrestrial atmosphere studies. Simulation studies of the Martian atmosphere can be accomplished by using a long path-absorption tube as described in the text. In this arrangement, a long path-absorption tube of the multiple-reflection type is filled with gas constituents which artificially simulate the Martian atmosphere. At one end of the tube, solar radiation, or a selected radiation source is introduced; at the other end, an infrared

spectrograph is connected. By varying the constituents of the artifical atmosphere as well as its physical conditions (temperature and pressure, particularly), a variety of spectrograms can be obtained. Comparison of such spectrograms with the spectrogram actually obtained from the Martian limb will provide knowledge of the composition of the Martian atmosphere. If the spectrograph of the edge of the Martian limb could be obtained, such a comparison will give the knowledge of the composition altitude profile of the Martian atmosphere. In addition, it is recommended that more work (experimental and theoretical) be done in obtaining reliable values of the cross sections and rate coefficients for the suspected reactions in the Martian atmosphere, under corresponding conditions. This is especially significant at the low predicted temperature (80°K) of the Martian ionosphere.

Experiments to investigate the nature and amount of polarized light given off by various combinations of solid carbon dioxide and water frost formed under the predicted temperature and pressure environment of the Martian polar caps should be performed.

Experimental and theoretical studies to determine the characteristic time constant for sublimation of CO_2 in the Martian upper atmosphere are recommended. Additional experimental and theoretical studies are needed to determine the thermal conductivity of the Martian surface and the convective heat transfer of the atmosphere near the surface.

DISTRIBUTION

DEP-A
Mr. Newby

R-DIR
Mr. Weidner

R-EO-DIR
Dr. Johnson (3)

R-ASO-DIR
Dr. Williams

R-AERO
Dr. Geissler
Mr. W. Vaughan
Mr. O. Vaughan
Mr. R. Smith
Mr. D. Weidner (50)
Mr. Dahm (2)
Mr. Felix (3)
Mr. Carter
Mr. H. Horn
Mr. Baker
Mr. McAnnally

R-SSL
Dr. Stuhlinger (3)
Dr. Shelton
Dr. Frary
Dr. Bucher

R-ASTR-DIR
Dr. Hauessermann

R-P&VE-DIR
Dr. Lucas (3)

External

Office of Space Sciences and Applications
NASA Headquarters
Washington, D. C. 20546
Dr. Fellows (2)

DISTRIBUTION (Continued)

External

Nortronics/Huntsville
Northrop Corporation
6025 Technology Drive
Huntsville, Alabama 35805
Mr. Stanley (10)
Dr. Chang
Mr. Lucas (2)
Mr. Youngblood (2)

Jet Propulsion Laboratory
4800 Oak Grove Drive
Pasadena, California 91103

National Aeronautics and Space Administration
Langley Research Center
Langley Station
Hampton, Virginia 23365

National Aeronautics and Space Administration
Goddard Space Flight Center
Greenbelt, Maryland 20771

Scientific and Technical Information Facility (25)
P.O. Box 33
College Park, Md. 20740
Attn: NASA Rep. (S-AK/RKT)